Practical Aspects of Modern Routine Solid-State Multinuclear Magnetic Resonance Spectroscopy: One-Dimensional Experiments

David L. Bryce,[†§] Guy M. Bernard,[§] Myrlene Gee,[†§] Michael D. Lumsden,[†]
Klaus Eichele,[†‡] and Roderick E. Wasylishen[†*]

Received: June 25, 2001
Accepted (in revised form): September 18, 2001

Abstract

New solid-state NMR (SSNMR) methods and applications continue to blossom such that a diverse array of physical, chemical, and biological problems are now being addressed using a variety of SSNMR experiments. While SSNMR is far from routine for chemists in the manner that a technique such as solution NMR is, there are nevertheless numerous applications of SSNMR which would be beneficial to many "non-specialists", e.g., synthetic chemists seeking to characterize their materials. This article gathers together practical details for those one-dimensional experiments which, in a broad sense, are considered "routine" in a modern SSNMR laboratory. Emphasis is placed on providing information and over 300 key references in a manner which will be useful for the novice and the non-specialist. For practicing SSNMR spectroscopists, it is hoped that this article will serve as a valuable reference in the laboratory. In addition to providing a brief review of pulsed Fourier transform NMR, the article discusses experimental details relating to the study of solid samples containing spin-$\frac{1}{2}$ nuclei, non-integer quadrupolar nuclei, and deuterium.

Published in:
Canadian Journal of Analytical Sciences and Spectroscopy **2001**, *46*, 46-82.
This document is not a reprint of this article, but has been typeset by the authors using the accepted manuscript, converted from WordPerfect to LaTeX 2_ε. Pagination and layout do not correspond to the printed version, but the content does (except for the omitted French abstract and the added table of contents) and includes the errata.

[†] Department of Chemistry, Dalhousie University, Halifax, Nova Scotia, Canada, B3H 4J3
[§] Department of Chemistry, University of Alberta, Edmonton, Alberta, Canada, T6G 2G2
[‡] Present address: Institut für Anorganische Chemie, Universität Tübingen, Auf der Morgenstelle 18, 72076 Tübingen, Germany
[*] Author to whom correspondence should be addressed. Phone: 780-492-4336, Fax: 780-492-8231,
Email: Roderick.Wasylishen@UAlberta.Ca, Web: http://ramsey.chem.ualberta.ca

Contents

1 Introduction and Overview

Solid-state nuclear magnetic resonance (SSNMR) spectroscopy is becoming increasingly important and accessible to the non-NMR specialist. At the same time, NMR spectroscopists are actively developing new techniques to address a large variety of problems relating to diverse areas of chemistry, physics, biology, biochemistry, materials science, and beyond. Perhaps one of the most appealing aspects of SSNMR is its ability to probe the structure and dynamics of so many different systems using such a wide assortment of NMR-active nuclei and experiments. The increasing popularity of SSNMR is reflected in Figure 1, which depicts the number of publications per year with keywords " 'solid state' and 'NMR' " as a function of year for 1989 through 2000, according to the Institute for Scientific Information's "Web of Science".[1]

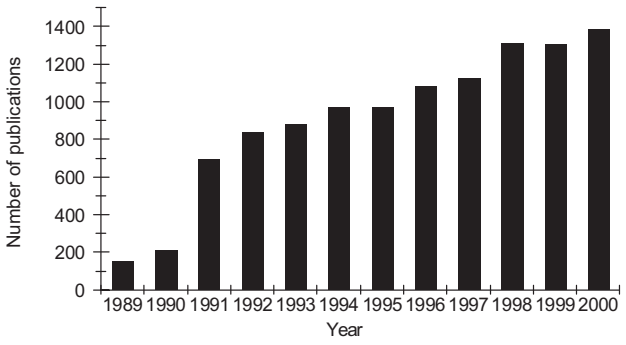

Figure 1: Plot of the number of publications per year for 1989-2000 based on a Web of Science search for keywords " 'solid state' and 'NMR' ".

The purpose of this article is to provide a practical reference guide for carrying out routine one-dimensional SSNMR experiments, or, at the very least, to provide references to relevant literature. This article is therefore aimed at two audiences. The first are the so-called "non-specialists", scientists who would benefit by incorporating simple SSNMR experiments into their research. The second group comprises established SSNMR research groups and their new graduate students who will be carrying out their research in the field of SSNMR, and who have the considerable task of sorting through textbooks and literature before carrying out their first experiments.

Progress in NMR is reviewed annually in many different serials, e.g., *Specialist Periodical Reports*, *Progress in NMR Spectroscopy, Annual Reports on NMR Spectroscopy, NMR: Basic Principles and Progress.* In particular, there are five volumes of the latter series which are devoted to solid-state NMR.[2] Valuable general[3,4] and specialized reviews relating to specific chemical systems, e.g., glasses and ceramics,[5,6,7] zeolites,[8] organic thin films,[9] proteins, peptides, and polypeptides,[10,11] coals,[12] and superconductors[13] are available. Dybowski provides short annual reviews of recent developments and applications in the field of SSNMR in *Analytical Chemistry*.[14] Early applications of solid-state NMR in chemistry were discussed in Fyfe's book "Solid-State NMR for Chemists".[15] Ripmeester and Ratcliffe have provided an informative introduction to the basics of SSNMR with an emphasis on applications in supramolecular chemistry;[16] Fitzgerald and DePaul have presented a useful overview of SSNMR of inorganic materials.[17] The aim of the present article is not to review the recent literature, but rather collect some of the most useful references for actually performing the experiments. In particular, the focus is limited to what we consider in a broad sense to be "routine" one-dimensional NMR experiments. Aside from deuterium, the relatively narrow topic of integer-spin quadrupolar nuclei such as ^{14}N is not addressed. It should be emphasized that two-dimensional experiments, e.g., many dipolar recoupling schemes,[18] are very important in solid-state NMR; however, these are not dealt with in the present paper.

The article is divided into the following sections: 2. A Brief Review of Pulsed Fourier Transform NMR; 3. Spin-$\frac{1}{2}$ Nuclei; 4. Non-Integer Quadrupolar Nuclei; 5. Deuterium NMR: A Powerful Technique for Probing Molecular Dynamics; 6. Synopsis; 7. Acknowledgements; 8. References. Most of the data presented were acquired on Chemagnetics CMX Infinity and Bruker AMX spectrometers; some were acquired on Bruker MSL and Varian Inova spectrometers. Spectra were simulated using the WSOLIDS NMR simulation package, which was developed in our laboratory.[19]

2 A Brief Review of Pulsed Fourier Transform NMR

2.1 Basic Components of NMR Spectrometers Designed to Investigate Solids

The purpose of this section is to describe the key components of a modern NMR spectrometer used to investigate solid samples. Emphasis will be placed on **differences** between spectrometers designed to study liquids and those designed to study solids. For further

details on basic NMR instrumentation, the interested reader is referred elsewhere.[20,21,22,23,24]

The majority of the fundamental design differences in a spectrometer used to study solids originate from the fact that the magnetic shielding experienced by a nuclear spin in a molecule varies with the orientation of the molecule with respect to the external applied magnetic field. In the solution phase, rapid random molecular tumbling averages the orientation dependence of the shielding to an isotropic value. However, in a crystalline powder sample, the NMR line shape results from the statistical distribution of all possible crystallite orientations and consequently will generally be much broader than for a solution sample. Furthermore, the presence of direct nuclear dipole-dipole interactions in solids, which are averaged to zero in solution, leads to an additional source of broadening.[25] Even for a stationary single crystal, the latter interaction will lead to NMR line widths which are generally much greater than in solution. For nuclei with spin $> \frac{1}{2}$, the quadrupolar interaction is often the dominant source of line broadening. Also, anisotropy in the bulk magnetic susceptibility of a solid sample results in some line broadening.[26] Therefore, the demands placed on external field stability for performing high-resolution NMR of solutions are relaxed for solid samples. In fact, dedicated solid-state NMR spectrometers often do not have a lock channel. However, this savings is more than offset by requirements for additional spectrometer components. Such requirements are discussed below.

2.1.1 High-Power Amplifiers

Due to the large spectral widths often encountered in SSNMR spectra, intense radiofrequency (rf) pulses are required on the spectrometer observe channel to excite uniformly the entire spectral range and produce distortion-free spectra. As well, due to the proton's large magnetic moment and ubiquitous presence in nature, direct dipolar couplings involving protons are often substantial (e.g., > 20 kHz for directly bonded ^{13}C-^{1}H) and require large amounts of rf energy to decouple. For example, in isotropic solutions where the dipolar interaction is averaged to zero, a decoupling power of a few Watts is generally sufficient to eliminate indirect X-H spin-spin (J) couplings whereas in the solid state, power requirements increase by approximately two orders of magnitude. For these reasons, the observe and decouple channels of a modern solid-state NMR spectrometer will typically each be equipped with a high-power amplifier capable of producing up to a kilowatt of power. These amplifiers will generally be linear class AB or nonlinear class C. For an excellent overview of the characteristics of these amplifiers, the reader is referred to two sets of notes.[27]

2.1.2 High-Speed Digitizer

In a modern pulsed Fourier transform (FT) NMR spectrometer, the free-induction-decay (FID) is digitized by an analogue-to-digital converter (ADC) before FT. One very important parameter characteristic of an ADC is its maximum sampling rate, as this defines the maximum resonance frequency range which can be properly digitized and, consequently, the largest spectral window. Since the NMR spectrum arising from nuclear spins in a powder sample often spans a very large frequency range, instruments for solids are generally equipped with high-speed digitizers capable of much faster sampling rates than spectrometers designed specifically to examine liquids. The tradeoff for these faster sampling rates is a reduced dynamic range. These considerations are particularly important for NMR investigations of quadrupolar nuclei, such as SATRAS experiments (see Section 4), where spectral windows in excess of 1 MHz are typical. As an example, the Bruker AMX 9.4 T solids instrument at Dalhousie University possesses a 12-bit ADC capable of digitizing spectral windows of up to 5 MHz whereas dedicated liquids instruments generally have 16-bit ADCs capable of observing a maximum spectral window of only 125 kHz.

2.1.3 Magic-Angle Spinning (MAS) Hardware and Equipment

A very large percentage of the research performed in the solid-state NMR field involves the investigation of powder samples which are spinning rapidly about an axis inclined at an angle of 54.74°with respect to the external applied magnetic field direction (see Section 3.2.2).[28,29,30,31,32] This angle, known as the magic angle, is that at which the spatial dependencies of many NMR interactions are averaged to their isotropic values. One notable exception to this is the second-order quadrupolar interaction, which is important for nuclei with spin $I > \frac{1}{2}$ (see Section 4). Not surprisingly, spinning a sample at a precisely defined speed and angle places further stringent design requirements on a solid-state NMR instrument. A critical component is the MAS speed controller which supplies the spinning gases as well as monitors and controls the spinning speed. Quite often the gas is compressed dry air; although, for low and high temperature experi-

ments, nitrogen gas should be used, especially to avoid oxidation at high temperatures. Some manufacturers recommend that nitrogen gas be used at all times in newer high-field probes. Modern MAS involves the application of two separate gas streams: *bearing* gas to support the sample, and *drive* gas to spin it. Currently, the maximum achievable spinning speed in a commercially available probe is about 35 kHz, for a rotor with an outer diameter of 2.5 mm. Modern MAS controllers have the ability to automatically spin samples at a desired speed. The parameters involved in automated spinning are built into the firmware of the controller and will vary with the size and wall thickness of the rotor and the design of the probe. Although this automated control generally works well, spinning particularly dense powders or half-full rotors can be troublesome and often one is best advised to manually control the spinning in such cases. Inert powders or inserts may be used to fill rotors, thereby facilitating stable spinning. Other simple improvements in spinning rate control have been presented by Chopin *et al.*[33]

2.1.4 High-Power Probes

Given the magnitude of the rf energy involved, as well as the requirement to spin solid powder samples rapidly, it should come as no surprise that high-power solid-state NMR probeheads are generally more complex than their low-power solution counterparts. This complexity results in greater space requirements for probe design and so traditionally solid-state NMR has been performed on wide-bore superconducting magnets with a bore diameter of 89 mm. However, in recent years, high-power probes for standard bore magnets (54 mm) have become available. Due to spatial restrictions, these standard-bore probes generally do not have triple-resonance or imaging capabilities. The field of solid-state NMR encompasses a tremendously diverse array of experiments, many of which place contradictory design requirements on a probe. Consequently, solids probes are generally designed with a given application or a closely related range of applications in mind and do not perform optimally when used outside this range. Probe design is beyond the scope of this review; the interested reader is referred to recent review articles by F. D. Doty.[34,35] We mention briefly that one should be aware of the quality factor, Q, of the sample coil (see Section 2.2).[36]

Without question, the most common probehead found in a solid-state NMR lab is a double-resonance probe capable of cross-polarization and MAS experiments in conjunction with high-power proton decoupling (see Section 3.2). The rotors which house the powder sample are typically made of zirconia or silicon nitride and are commercially available in sizes with outer diameters ranging from 2.5 to 14.0 mm. With MAS experiments, air friction in the bearings can lead to substantial temperature increases. For example, at MAS rates of 35 kHz, temperature increases up to 50 K above room temperature have been measured.[37] Since all NMR interactions are temperature dependent, this sample heating phenomenon must be considered when performing fast MAS experiments (see Section 3.3 for further details). Another important consideration related to heat production involves the application of high-power proton decoupling. Although MAS will help in dissipating the heat produced from the rf decoupling energy, it is important to also use an ambient temperature flush gas for this purpose. Furthermore, sufficiently long relaxation delays must be used, particularly when performing experiments on static samples with these probes. For stationary samples, acquisition times are invariably less than 100 ms. To keep the duty cycle low when ^{1}H decoupling for such time periods, we commonly use a minimum relaxation delay of at least a few seconds when acquiring spectra of stationary samples, even when the T_1 of the relevant nuclei is much shorter than this. Finally, it is noted that these probeheads are manufactured to cover a variety of frequency ranges dictated by the user. Tuning can be accomplished in a variety of ways such as with a sweep generator or a tuning bridge. However, our method of choice is to minimize the reflected power from the probe using an oscilloscope and an appropriate directional coupler in-line between the preamp and the probe.[38]

Other less-commonly used probes found in solid-state NMR laboratories include those designed to study single-crystal samples, "wideline" probes optimized for the investigation of static powder samples, CRAMPS probes for studying abundant spins (^{1}H, ^{19}F) (see Section 3.4), triple resonance probes, and more recently developed HFXY quadruple resonance probes.

2.2 Data Acquisition and Processing Free-Induction Decays

Given the magnitude of rf energy involved in solid-state NMR experiments as well as the complexity of many of the experimental techniques, the solid-state NMR spectroscopist must become intimately acquainted with the spectrometer to become an efficient

and effective user. The "black box approach" will almost always ultimately lead to disaster and hence to very costly repairs and spectrometer down-time. The intensity of the B_1 fields are most often quantified in the NMR literature according to the frequency of the induced magnetization precession:

$$\omega_1 \;=\; 2\,\pi\,\nu_1 \;=\; \gamma B_1 \qquad (1)$$

Since the flip angle, θ, (in radians), is given by:

$$\theta \;=\; \omega_1 t_{\rm p} \qquad (2)$$

where $t_{\rm p}$ is the pulse width, it is easy to show that for a $\pi/2$ pulse, the radiofrequency field, ν_1, is given by:

$$\nu_1 \;=\; \frac{1}{4t_{\pi/2}} \qquad (3)$$

Thus, a 5 μs $\pi/2$ pulse width corresponds to a 50 kHz rf field. Since solid-state NMR experiments are generally conducted using less than the maximum available power, it is obviously very important to be able to adjust the strength of the applied rf fields. For example, one of the most common solid-state NMR techniques, cross-polarization, involves the adjustment of the B_1 fields on the observe and the proton channel until a Hartmann-Hahn match[39] is achieved (see Section 3.2.1). Power adjustment is generally performed on a modern solid-state spectrometer by attenuating the input to the high-power amplifiers via software. The unit of attenuation is the decibel (dB)[20] and is defined in terms of a logarithmic scale of power ratios, $P_{\rm f}/P_{\rm i}$, where $P_{\rm i}$ is the initial power and $P_{\rm f}$ is the final power:

$$dB \;=\; 10\,\log_{10}\,(\,\frac{P_{\rm f}}{P_{\rm i}}\,) \qquad (4)$$

Furthermore, since power is proportional to the square of the voltage, V, at a fixed impedance and since the intensity of the rf fields is proportional to the voltage applied across the probe sample coil, a more useful definition for the NMR spectroscopist is:

$$dB \;=\; 20\,\log_{10}\,(\,\frac{V_{\rm f}}{V_{\rm i}}\,) \qquad (5)$$

For example, if the operator decided that a particular pulse width needed to be lengthened by a factor of two, this would necessitate reducing the rf field by a factor of 2 ($V_{\rm f}/V_{\rm i} = 0.5$) and from eq. 5, a further 6.0 dB attenuation would be required. Additionally, suppose a 4 dB attenuator needs to be inserted in-line before the probe for a particular experiment. Again, making use of eq. 5, the operator can expect rf field strengths to decrease and hence pulse widths to lengthen by a factor of 1.6.

Not only does the spectroscopist have to be aware of the amount of rf energy being applied but also how long it is applied, which is in turn dictated by the ability of the particular component (*i.e.*, probe, amplifier, filter, etc.) to dissipate the heat produced. For continuous wave (CW) operation, the power handling capabilities of the component are specified simply by a safe maximum power whereas with pulsed rf the length of time the power can be applied must also be defined. For example, the specification sheet for one of our high-power CP/MAS probes indicates that the maximum decoupler rf field strength is ≈90 kHz which should be applied for no more than 50 ms. Similar arguments hold true for pulsed amplifiers, although specifications are normally given in combination with a maximum duty cycle,[40] which represents the fraction of time the amplifier is on during an experiment. Amplifiers that have a maximum pulse power of 1 kW generally have a duty cycle less than 10%. Thus, application of a 10 μs pulse dictates that the total time for a single scan, including the recycle delay, must be ≥100 μs.

Since many experiments involve the application of high-power proton decoupling during the acquisition time, AT, this parameter takes on an even greater significance in SSNMR and must be thoroughly understood. The approach in high-resolution solution NMR where one typically leaves on the proton decoupler throughout the experiment for nOe enhancement purposes and digitizes the FID for periods of a second or more must be abandoned in the solid state! As mentioned earlier, the NMR FID is digitized by an ADC which outputs a binary number proportional to the size of the voltage at its input. A very important parameter associated with this digitization process is the length of time between sampled points, known as the dwell time, DW. The importance lies in the fact that DW determines the largest resonance frequency relative to the transmitter frequency which can be accurately digitized and hence the maximum spectral width, SW.[41,42,43] High-speed digitizers found on SSNMR spectrometers are capable of short dwell times and hence large spectral widths. The relationship between DW and SW originates from the Nyquist theorem which states that the sampling rate must be greater than or equal to twice the maximum resonance frequency (Nyquist frequency, NF).[41,42,43]

$$sampling\ rate \;=\; \frac{1}{DW} \;=\; 2NF \qquad (6)$$

For the case of single-channel acquisition, which applies to the following discussion, NF is equivalent to the total SW. It is straightforward to understand that the acquisition time (AT) is given by DW multiplied by the number of time-domain points collected, TD:

$$AT = (TD)(DW) = \frac{TD}{2NF} = \frac{TD}{2SW} \quad (7)$$

It is also very important to recognize that the AT determines the digital resolution, DR (units of Hz/point), of the NMR spectrum:[41,42,43]

$$DR = \frac{1}{AT} = \frac{2SW}{TD} \quad (8)$$

Therefore, one can improve the digital resolution of the spectrum by lengthening the acquisition time through either decreasing the spectral width or increasing the number of data points.[44] An improvement in digital resolution thus comes at a price: longer experimental times and hence a loss in sensitivity. For example, if one wishes to digitize a line width or a line separation of 100 Hz, an AT of at least 10 ms is required. The solid-state NMR spectroscopist must be cognisant of the fact that longer acquisition times often mean longer applications of high-power proton decoupling. Thus, as a **rough** rule-of-thumb, a digital resolution of better than about 4 Hz/point is generally not practical at typical decoupling field strengths of 75 kHz (AT $<$ 250 ms). The actual maximum safe decoupling field and AT will be determined in part by the diameter of the rf coil; smaller coils can withstand more power over a given AT. It is also worth mentioning that one might anticipate that using TD points to characterize a given SW would result in a DR of SW/TD rather than the result given in eq. 8. The factor of two arises from the fact that FT yields a real and imaginary spectrum with $TD/2$ points each (single-channel acquisition). The presence of these two spectra are required for phasing purposes such that the absorption and dispersion mode spectra can be produced.

Modern NMR spectrometers employ a method of detection called *quadrature detection* which involves the use of two phase-sensitive detectors with reference inputs which are 90°out-of-phase with each other.[41,42,43] The primary advantage over a single detector is the ability to determine sign information, enabling the transmitter frequency to be placed in the middle of the spectral window rather than at one edge.[22] This technique also leads to further performance advantages, e.g., signal-to-noise improvements of $\sqrt{2}$, which are well documented.[43,45] One approach is to sample two data points *simultaneously* after each dwell period, one from each detector, resulting in a complex data pair.[45] After acquisition, the complex data are subject to a complex FT rather than the so-called real FT performed on the real data obtained with single-phase detection.[46] Calculating acquisition times based on data collected using simultaneous quadrature detection is potentially confusing and best illustrated with an example. Suppose the spectroscopist wishes to collect a ^{13}C spectrum using a total spectral range of 250 ppm, or 25 kHz at 9.4 T, using 4K total data points. With single-detection, the NF is 25 kHz so it is necessary to sample at 50 kHz ($DW = 20$ μs). Using eq. 7, the AT is calculated to be 81.92 ms. If we switch to simultaneous quadrature detection, we halve the Nyquist frequency to 12.5 kHz and therefore we must now sample at 25 kHz ($DW = 40$ μs). Also, 4K total data points now represent 2K complex data pairs so that $AT = 2\text{K} \times 40$ μs $= 81.92$ ms, the same result. There is a second method of quadrature detection known as sequential acquisition in which data points are sampled at the two detectors sequentially rather than simultaneously. This approach is used frequently on Bruker instruments as well as in 2D NMR and is described in detail elsewhere.[42,45,47,48]

A concept common to all FT NMR with which the solid-state NMR spectroscopist must be familiar is aliasing or the folding of peaks due to an inadequate rate of digitization (sampling rate $< 2NF$). An aliased peak lies outside of the spectral window but within the filter window (FW) and can be identified by its phase properties and frequency dependence on the transmitter placement. It is useful to know that folded peaks arising from data collected with simultaneous quadrature fold about the opposite end of the spectrum, whereas the folding occurs about the same edge of the spectrum for data collected with sequential acquisition (as well as single detection).[45]

In concluding this section, a few comments about pulse widths are in order. Accurate calibration of pulse widths is obviously an extremely important prerequisite to the success of many SSNMR experiments. Keifer's article discusses several aspects of utilizing pulse width arrays for pulse width calibrations,[49] e.g., off-resonance effects, B_1 inhomogeneity. In solids, calibration of pulses is most often carried out by directly observing the spins, whereas in solution indirect methods such as INEPT are frequently used. For the case of $I = \frac{1}{2}$ nuclei and for a given power level, the magnetization flip angle varies sinusoidally with the pulse width according to eq. 2 with maximum signal occurring at

$\theta = \pi/2$, a null at $\theta = \pi$, etc. Since the derivative of the sine function is greater at $\theta = \pi$ than at $\pi/2$, it is advisable to determine the π pulse width first and calculate the other necessary pulse widths based on this result. Note that in practice the π pulse usually does not produce a clean null but rather a dispersive peak due to rf inhomogeneity effects and so the π pulse criterion becomes zero peak area rather than intensity. Also note that it is important when measuring pulse widths to minimize off-resonance effects (position the transmitter close to on-resonance) as well as to leave an adequate delay between pulses for spin-lattice relaxation to occur. Under normal circumstances, the spectroscopist will have some idea of what pulse widths to expect for a given power before starting the pulse width calibration, although this will not always be the case. If not, it is advisable to first use substantial attenuation and measure the power using either a scope or wattmeter. Once it has been confirmed that this rf can be handled safely by the probe, the pulse width calibration may proceed. Finally, eqs. 4 and 5 may be used to adjust the attenuation and therefore the pulse width to within the desired range.

An extremely important concept related to pulse widths, particularly in the field of solid-state NMR, is the excitation profile of a pulse. Even though the output of the rf source in an NMR spectrometer is a CW signal at a fixed carrier frequency, the fact that the transmitter gates this rf on and off to produce a square pulse results in a range of excitable frequencies centred about the source frequency. To a good approximation, this range is determined by taking the FT of the square pulse in the time domain and results in an excitation profile described by the $(\sin x)/x$ or sinc x function. In fact, the only frequencies not contained within this profile occur at integer multiples of $1/PW$ so that the bandwidth contained between the first nodes of a 10 μs pulse will be 200 kHz ($\pm$100 kHz). A shorter PW excites a greater bandwidth than a longer pulse. The problem is that the sinc x function varies in amplitude over the bandwidth so the 200 kHz range is excited to varying degrees of efficiency and the resulting spectrum is severely distorted. Thus, in practice, to excite the complete spectral range as uniformly as possible, it is necessary to make $1/PW$ much larger than the SW so that only the relatively flat central portion of the profile is used to excite the spectrum. As a *rough* guide, it is good practice to set the pulse width such that the spectrum of interest does not extend over a spectral region which exceeds $\pm 1/4PW$. In solid-state wideline NMR experiments where SW can be easily on the order of 1 MHz, this places considerable demands on the spectrometer electronics since enough power must also be applied to produce the desired flip angle at these short pulse widths. Knowledge of the probe quality factor, Q, is also very important for obtaining reliable spectra over a wide spectral window. Q may be measured as the Larmor frequency divided by the full-width half maximum (or minimum) of the tuning curve. Jiang has also described an alternative method for measuring Q.[36] Qualitatively, a smaller value of Q allows one to observe a larger spectral window without significant distortion. Adjustment of the match away from its optimum setting will influence the value of Q to some extent.

3 Spin-$\frac{1}{2}$ Nuclei

3.1 Stationary Samples

3.1.1 Powder Samples

For an isolated spin-$\frac{1}{2}$ nucleus, the major source of line broadening, in general, is the chemical shift anisotropy. The chemical shift interaction is described by a second-rank tensor with three principal components $\delta_{11} \geq \delta_{22} \geq \delta_{33}$ where δ_{11} is the chemical shift when the applied magnetic field, B_0, is along the direction of least shielding, and δ_{33} is the chemical shift when B_0 is aligned with the most shielded direction. Alternatively, the line shape can be described by three derived parameters: the isotropic chemical shift, $\delta_{\rm iso}$, the span, $\Omega = \delta_{11} - \delta_{33}$, which is the breadth of the chemical shift tensor, and the skew, $\kappa = 3(\delta_{22} - \delta_{\rm iso})/\Omega$, which describes the shape of the powder pattern.[50] These are the recommended conventions for reporting the chemical shift tensor, although the reader should be aware that other conventions are frequently used in the literature.[50]

More commonly, a spin-$\frac{1}{2}$ nucleus is near another spin-active nucleus; hence, direct dipolar spin-spin coupling also contributes to line broadening. The splitting arising from the dipolar interaction is $R\,(3cos^2\theta - 1)$ for heteronuclear spin pairs and $3R\,(3cos^2\theta - 1)/2$ for magnetically equivalent homonuclear spin pairs, where the dipolar coupling, R, is $(\mu_0/4\pi)\gamma_1\gamma_2(\hbar/2\pi)\langle r^{-3}\rangle$, and r is the distance between the two dipolar coupled nuclei.[25] For an AX spin pair comprised of like nuclei, the "heteronuclear" equation applies. The angle θ describes the orientation of the internuclear vector with respect to B_0. In a microcrystalline sample, all values of θ are present and a powder pattern is observed. For most samples containing abundant spins (^{1}H or ^{19}F), strong dipo-

lar coupling contributes significantly to the line width of the spectrum. For quadrupolar nuclei ($I > \frac{1}{2}$), the nuclear quadrupolar interaction also contributes to the line width, and is generally the major contributor. The NMR spectra of quadrupolar nuclei will be discussed in Section 4.

NMR spectra of stationary samples are of particular interest when the isolated spin or spin pair approximations hold. For spin-$\frac{1}{2}$ nuclei, spectra of stationary powder samples will yield information about the chemical shift tensor, and, in the case of a spin pair, additional information concerning the direct (**D**) and indirect (**J**) spin-spin coupling tensors. The dipolar-chemical shift method[51,52,53,54] has been widely used to provide not only the information indicated above, but also the relative orientations of the chemical shift tensors of the two spins.[55] This information is typically extracted by spectral simulations. Problems may arise when the breadth of the powder pattern is large (> 50 kHz). The first consideration is that of uniform excitation across the spectrum (see Section 2.2). A second consideration is the probe "dead time". Long dead times will result in significant line shape distortions. In such cases, it is possible to employ a Hahn echo ($\pi/2\ -\tau\ -\pi\ -\tau$)[56] or a Carr-Purcell Meiboom-Gill echo[57] for an isolated spin or heteronuclear spin pair.[58,59] Such an echo refocuses inhomogeneity in the external applied magnetic field as well as the chemical shift and heteronuclear spin-spin coupling. The homonuclear spin-spin couplings are not refocused for a homonuclear spin pair,[41] and hence a "solid echo"[32] should be used rather than a Hahn-type echo for such systems. Rance and Byrd[60] describe how best to obtain spin-$\frac{1}{2}$ powder spectra using phase-cycled Hahn echo techniques. For ^{13}C, where the chemical shift range is relatively small, excellent spectra can usually be acquired without using an echo, particularly at applied magnetic field strengths less than 10 T. An example of a case where the chemical shift anisotropy is the dominant influence on the appearance of the spectrum is shown in Figure 2 for phenylacetic-*carboxy*-^{13}C acid (99% enriched). From this spectrum, accurate values for the principal components of the chemical shift tensor can be ascertained. An example of a spectrum of a stationary dipolar-coupled spin pair is given in Figure 3.[61]

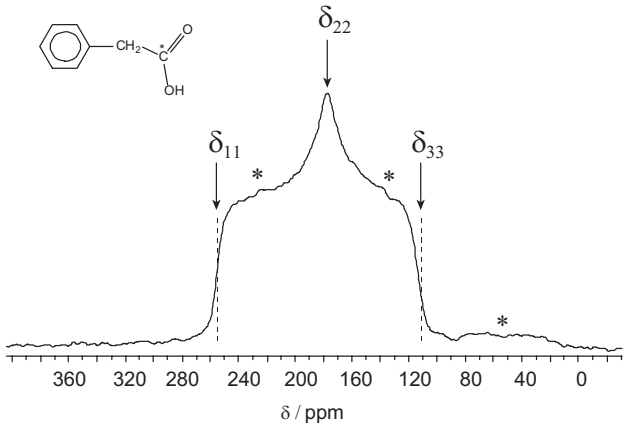

Figure 2: C-13 CP spectrum of a stationary sample of singly-labelled (99%) phenylacetic-*carboxy*-^{13}C acid ($B_0 = 4.7$ T, $\nu_L = 50.3$ MHz, number of acquisitions = 256) acquired with TPPM decoupling (see Section 3.2.3). There are six aromatic carbons in this compound, and in natural abundance they contribute to the powder pattern. Some of these distortions are indicated by asterisks. The principal components of the labelled carbon chemical shift tensor are determined from the powder pattern as indicated ($\delta_{11} = 257$ ppm, $\delta_{22} = 176$ ppm, $\delta_{33} = 110$ ppm).

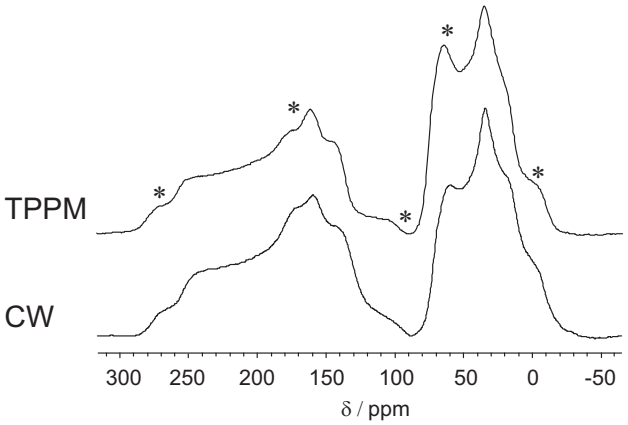

Figure 3: C-13 CP spectra of doubly-labelled (99%) phenylacetic-$^{13}C_2$ acid ($B_0 = 4.7$ T, $\nu_L = 50.3$ MHz, number of acquisitions = 1024). Chemical shift anisotropy and ^{13}C-^{13}C dipolar coupling account for the features of the observed line shapes. In the bottom trace, CW proton decoupling was used; this leaves some features poorly resolved. In the top trace, however, two-pulse phase-modulated (TPPM, see Section 3.2.3) decoupling leads to an improvement in the definition of the discontinuities in the spectrum. Spectra were otherwise acquired under identical conditions. Asterisks indicate particular features of the lineshape which are more clearly defined as a result of the TPPM decoupling.

3.1.2 Single Crystals

NMR studies of single crystals are ideal for the unambiguous characterization of interactions that are described by second-rank tensors, for example the chem-

ical shift, the direct (dipolar, **D**) and indirect (**J**) coupling, and the electric field gradient for quadrupolar nuclei (Section 4). As well, this technique is invaluable in situations where multiple crystallographically and/or magnetically nonequivalent sites hinder the straightforward analysis of the NMR spectra of powders. Unfortunately, this experiment is not performed often because single crystals of adequate size and quality are difficult to obtain. In addition, any imperfections such as cracks or twinning are difficult to deal with. Several good references for growing single crystals are available.[62,63,64] Vosegaard *et al.* have recently described successful experiments using relatively small crystals and small rf coils.[65] Single crystals, preferably with dimensions of at least 1 mm, are mounted in a three sided cube which is inserted into a goniometer in the single crystal probe. In the most common design, the crystal is rotated about an axis perpendicular to the applied magnetic field. Generally, it is necessary to perform rotations of the crystal about the three axes of the cube, although methods have been developed which require rotation only about two axes which are not mutually perpendicular.[66,67,68,69,70] NMR spectra are acquired for a series of angles for each rotation.

Presented in Figure 4 are ^{31}P spectra of tetramethyldiphosphine disulfide, obtained on a Chemagnetics CMX Infinity 200 spectrometer with a Doty single crystal probe. Analysis of the peak positions as a function of the rotation angle provides the principal components of the chemical shift tensors as well as information about the orientations of the tensors in the molecular framework. Details of this analysis may be found in the literature.[71] While the interaction tensors are completely characterized in most cases, one should be aware of difficulties in assigning the tensors to particular sites in the crystal, for example when there are several magnetically nonequivalent sites in the single crystal and no special symmetry associated with the sites to limit the possible tensor orientation. These subtleties are discussed in more detail elsewhere.[72] We emphasize that single-crystal studies are by no means limited to spin-$\frac{1}{2}$ nuclei; selected applications to quadrupolar nuclei will be discussed briefly in Section 4.

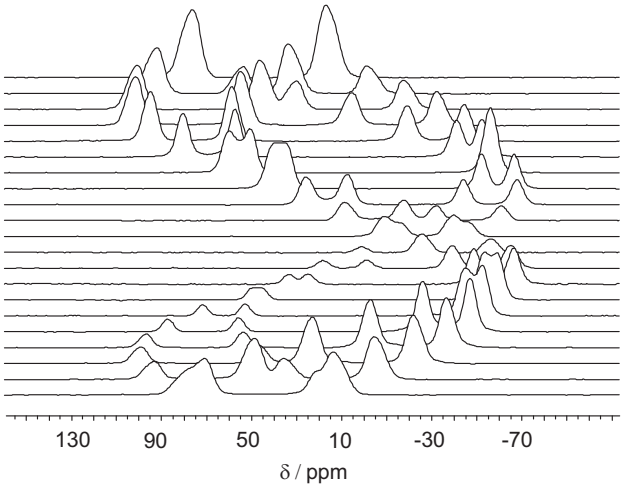

Figure 4: Phosphorus-31 CP NMR spectra of a single crystal of tetramethyldiphosphine disulfide as a function of crystal orientation in the applied magnetic field, obtained on a Chemagnetics CMX Infinity 200 spectrometer (B_0 = 4.7 T) using a Doty 4 mm single-crystal NMR probe. The rotation angle was incremented by 9° for each experiment, and 64 transients were added for each spectrum.

3.2 "High-Resolution" CP/MAS NMR Spectroscopy

One goal of SSNMR spectroscopists is to obtain "solution-like" spectra for solid samples. To obtain high-resolution NMR spectra of dilute spin-$\frac{1}{2}$ nuclei in solid samples, usually three techniques are combined:[32,73] (*i*) cross-polarization (CP) from abundant spins (typically but not necessarily ^{1}H or ^{19}F),[31,39,74,75,76,77,78,79,80,81] (*ii*) magic-angle spinning (MAS),[31,82,83,84,85,86,87] and (*iii*) high-power heteronuclear decoupling.[88,89,90,91,92] We note that CP and high-power decoupling are techniques which are also generally applied to spectra of stationary powder samples and single crystals (Section 3.1); however we present these methods in the context of high-resolution CP/MAS experiments.[93]

3.2.1 Cross-Polarization: Transferring Magnetization

CP allows the dilute spins to borrow magnetization from the abundant spins. In principle, CP results in a signal enhancement given by $\gamma_{\mathrm{I}}/\gamma_{\mathrm{S}}$, where γ_{I} is the magnetogyric ratio of the abundant spin and γ_{S} is that of the dilute or rare spin. Shown in Table 1 are the values of this ratio for a representative series of dilute spin-$\frac{1}{2}$ nuclei, with ^{1}H as the I spin. Equally important is the reduction in the recycle time between radiofrequency pulses. CP allows one to use recycle delays on the order of the I spin T_1 instead of the S spin T_1. Since typically the S spin T_1 values are long, this reduction can often be many orders of magnitude, and allows for the acquisition of a spectrum with an improved

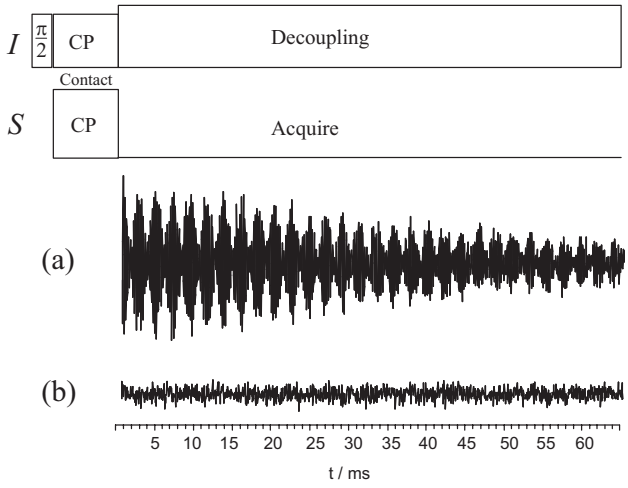

Figure 5: Pulse sequence for single-contact matched cross-polarization, with decoupling on the I channel. The pulses are not to scale, e.g., the $\pi/2$ pulse is typically on the order of μs and the contact time is on the order of ms. After the I-spin $\pi/2$ pulse, there is a 90 degree phase shift in the I-spin magnetization (*i.e.* a spin-locking pulse is applied on the I channel during CP). Shown in (a) and (b) are the free-induction decays (FIDs) for ^{13}C CP/MAS spectra of adamantane ($B_0 = 4.7$ T, $\nu_{\rm L} = 50.3$ MHz, number of acquisitions = 8, recycle delay = 5 s, contact time = 6.5 ms, $\nu_{\rm rot} = 2$ kHz). In (a), the Hartmann-Hahn condition is satisfied and the FID signal continues ringing longer than the 65 ms shown here. In (b), the Hartmann-Hahn match is not satisfied. The advantages of using CP are clearly apparent. Adamantane is particularly mobile in the solid state; hence, the ^{13}C linewidth is narrow and the FID extends out for a relatively long time. For many solid samples, an acquisition time of 50 ms is adequate to avoid truncating the FID.

signal-to-noise ratio for a given amount of experiment time. The reader should be aware that for solid samples, generally $T_1 > T_2$, which is not in the extreme narrowing region, unlike many situations in solution NMR. Thus, when dipole-dipole relaxation is dominant, T_1 will scale with B_0^2. The most common form of CP is known as Hartmann-Hahn CP[39] or "single-contact matched CP" (Figure 5). When setting up a CP experiment, one must ensure that the well-known Hartmann-Hahn match condition is satisfied:

$$\gamma_{\rm I} B_{1\rm I} = \gamma_{\rm S} B_{1\rm S} \qquad (9)$$

This condition is usually achieved experimentally by keeping the power on the I channel constant while adjusting the power level on the S channel so that the most intense S spin spectrum is observed.

Shown in Table 1 are recommended samples for establishing the Hartmann-Hahn match for a variety of nuclei.[75,94,95,96,97,98,99,100,101,102,103,104,105] For ^{13}C, adamantane[93,106] and glycine[107] are two commonly used secondary external reference compounds. Unfortunately, the use of glycine can lead to complications due to polymorphism.[107] Presented in Figure 5 are two FIDs for naturally-abundant ^{13}C in adamantane. The Hartmann-Hahn condition is satisfied in (a), but not in (b). It should be noted that the carbon-proton dipolar interactions in adamantane are easily averaged by moderate MAS rates due to rapid molecular reorientation of the molecules within the crystal lattice. Thus, if adamantane is to be used for setting up CP experiments, MAS rates of no more than approximately 2 kHz are recommended.

The rf fields which are associated with the B_1 magnetic fields are turned on for a period known as the contact time, or mixing time, which is on the order of milliseconds (Figure 5). It is during this time that magnetization is transferred from the I spins to the S spins. The degree to which the S spins have been magnetized depends on the contact time. The rate of CP is initially governed by $T_{\rm IS}$, a time constant which is proportional to the second moment[20,41,108] of the dipolar coupling between the I and S spins.[32] At longer contact times, however, spin-lattice relaxation of the I spins in the rotating frame ($T_{1\rho}$) dominates. As an example, plots of the integrated relative intensity of the cross-polarized ^{1}H→^{15}N signal of normal and N-deuterated samples of 1-methoxy-4-(N-phenylamino-methyl) naphthalene acquired under conditions of MAS are shown in Figure 6.[59] Fitting of this type of data yields the time constants $T_{\rm IS}$ and $T_{1\rho}(^1{\rm H})$.[59]

It is possible, if $T_{1\rho}$ is sufficiently long, to use multiple-contact matched CP.[32] The worst scenario is a long $T_1(I)$ and a short $T_{1\rho}(I)$. A FLIPBACK pulse can be used to increase the number of acquisitions when the I spin T_1 values are long.[109] Alemany *et al.*[110] have studied a series of model highly protonated organic compounds and determined that a contact time of 2.25 ms (^{13}C/^{1}H) gives rise to ^{13}C spectra which may be integrated to give atomic site ratios. Although there are very specific cases where quantitative information may be extracted,[111] the reader should be aware that in general, *spectra obtained with CP cannot be integrated quantitatively.*

Sebald's review[75] provides details concerning the application of CP/MAS to "less common" spin-$\frac{1}{2}$ nuclei: ^{77}Se, ^{89}Y, ^{109}Ag, ^{113}Cd, ^{119}Sn, ^{125}Te, ^{183}W, ^{195}Pt, ^{199}Hg, and ^{207}Pb. As expected, contact times

Table 1: Enhancement factors, γ_I/γ_S, as a result of CP from ^{1}H for some spin-$\frac{1}{2}$ nuclei and CP set-up samples.

Dilute spin	γ_{1H}/γ_S	Set-up Sample
^{13}C	3.98	adamantane; polydimethylsilane (106b); glycine
^{15}N	−9.86	$^{15}NH_4NO_3$
^{19}F	1.06	[a]
^{29}Si	−5.03	$(CH_3)_3Si(CH_2)_2COONa$; $(CH_3)_3Si(CH_2)_3SO_3Na$ (105b)
^{31}P	2.47	$NH_4H_2PO_4$ (103)
^{77}Se	5.22	$(NH_4)_2SeO_4$ (98)
^{109}Ag	−21.4	$[CH_3CHC(OH)COO]Ag$ (95,75)
^{113}Cd	−4.48	$Cd(NO_3)_2.4H_2O$ (101, 102)
^{119}Sn	−2.67	$Sn(C_6H_{11})_4$ (96,99)
^{125}Te	−3.14	$Te(OH)_6$(97)
^{129}Xe	−3.59	[a]
^{195}Pt	4.58	$K_2Pt(OH)_6^{b)}$ (100); $(NH_4)_2PtCl_6$ (104)
^{199}Hg	5.52	$(NEt_4)Na[Hg(CN)_4]$; $(NBu_4)_2[Hg(SCN)_4]$ (94)
^{207}Pb	4.79	$Pb(p\text{-tolyl})_4$; $PbPh_4$ (99)

[a] Most ^{19}F and ^{129}Xe CP/MAS experiments are set up directly on the sample of interest. [b] It has been suggested that the lead CP/MAS standards are also suitable for setting up ^{195}Pt experiments due to the close resonance frequencies of ^{207}Pb and ^{195}Pt (99).

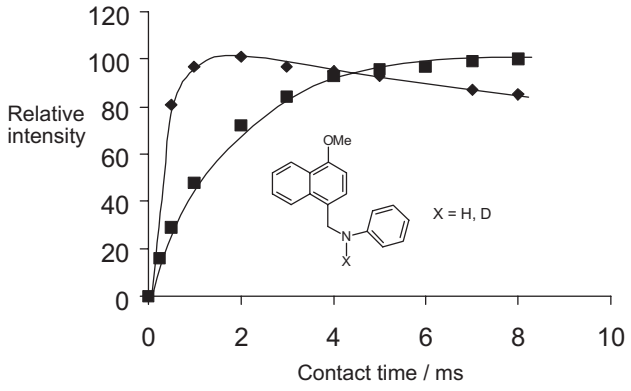

Figure 6: Plots of the ^{15}N isotropic signal intensity as a function of contact time (CP from protons) for MAS samples of normal (♦) and *N*-deuterated (■) 1-methoxy-4-(*N*-phenylamino-methyl) naphthalene.

become longer for low-γ nuclei. For example, the optimum contact time for ^{109}Ag CP/MAS in silver lactate is on the order of 50 ms.[75,95] Reviews specific to SS-NMR of mercury compounds are also available.[112,113] CP from ^{19}F to spin-$\frac{1}{2}$ nuclei, while much less common than CP from protons, is feasible, e.g., ^{19}F→^{13}C, ^{19}F→^{29}Si and ^{19}F→^{119}Sn experiments have been carried out.[114,115] It is also possible to carry out double CP experiments,[116] e.g., ^{1}H→^{13}C→^{15}N; this technique may be used, for example, to observe only ^{15}N nuclei which are close in space to ^{13}C nuclei.

Difficulties encountered when MAS is combined with CP are discussed in the following section. We emphasize again that there is no requirement for CP to be combined with MAS; CP is also commonly used for acquiring spectra of stationary samples.

3.2.2 Magic-Angle Spinning and CP

As briefly mentioned in Section 2.1.3, MAS involves rapidly spinning a sample about an axis inclined at $\arccos(1/\sqrt{3}) = 54.7356^\circ$ relative to the external applied magnetic field, B_0. The main advantage of MAS as it pertains to the acquisition of high-resolution spectra of dilute spin-$\frac{1}{2}$ nuclei is that the chemical shift tensor associated with a particular nucleus is averaged to its isotropic value; this allows for chemical shift resolution. In practice, it is often the case that MAS rates are not sufficiently large compared to the span of the chemical shift tensor. This leads to a series of peaks, spaced at integer multiples of the MAS rate from the isotropic peak, which are known as *spinning sidebands* (ssbs). The isotropic peak is not necessarily the most intense one. It is very important to have a constant spinning rate; the n^{th} order ssb will have a line width due to variations in the MAS rate of $n(\Delta\nu_{\text{rot}})$, where $\Delta\nu_{\text{rot}}$ is the variation in the MAS rate. While high MAS rates reduce the number of ssbs and increase the signal-to-noise, sufficiently rapid spinning

may lead to difficulties in achieving the Hartmann-Hahn match.[93,117] Briefly, the cause of this problem is related to the fact that as the MAS rate increases, it averages the *II* and *IS* dipolar couplings as it becomes comparable in magnitude to the strength of these couplings. A number of techniques have been developed to alleviate this problem. These include variable-amplitude CP (VACP),[118,119] ramped-amplitude CP (RAMP CP),[120] rotor-synchronized amplitude modulation CP (AMCP),[80,81] simultaneous phase inversion CP (SPICP),[121] radiofrequency-driven recoupling in CP (RFDRCP),[122] and variable-effective-field CP (VEFCP).[123] Shown in Figure 7 is a demonstration of the utility and effectiveness of VACP. Spectrum (A) is a ^{13}C CP/MAS spectrum of 99% doubly-labelled Ph^{13}CH$_2$^{13}COOH,[61] while spectrum (C) was obtained using the VACP pulse sequence. Both spectra were acquired at an MAS rate of 12576 Hz. Clearly, a significant improvement in signal-to-noise results. Note that the two carbons benefit to differing degrees, since they are dipolar-coupled differently to the protons in the molecule. A relatively new pulse sequence for improving CP under conditions of MAS is amplitude-modulated adiabatic-passage CP (AMAP-CP).[79] In theory, this should be the most effective and robust CP technique reported to date.

The isotropic peak may be readily differentiated from the ssbs because unlike the ssbs, its position is independent of the spinning rate. Although ssbs complicate the appearance of a spectrum and result in a loss of intensity of the isotropic peak, there is useful information which may be gained from the ssbs. Consider an isolated spin, as is approximately the case under conditions of high-power proton decoupling, in PhCH$_2$^{13}COOH. Two techniques which may be used in such a case to extract the principal components of the ^{13}C chemical shift tensor are Herzfeld-Berger analysis[124] and the method of moments.[125] Presented in Figure 8 is a ^{13}C CP/MAS spectrum of PhCH$_2$^{13}COOH. The MAS rate is deliberately relatively slow, so that many sidebands are apparent. Employing the method described by Herzfeld and Berger[124] yields the principal components of the carbonyl carbon chemical shift tensor.[61] The analysis depends on knowledge of the relative intensities of the various spinning sidebands. An MAS technique for producing spectra with peaks representing the principal components of the chemical shift tensor has been proposed;[126] this method should be most useful when homonuclear dipolar couplings are much less than the span of the chemical shift tensor (in Hz).

For an isolated spin, the elimination of ssbs is

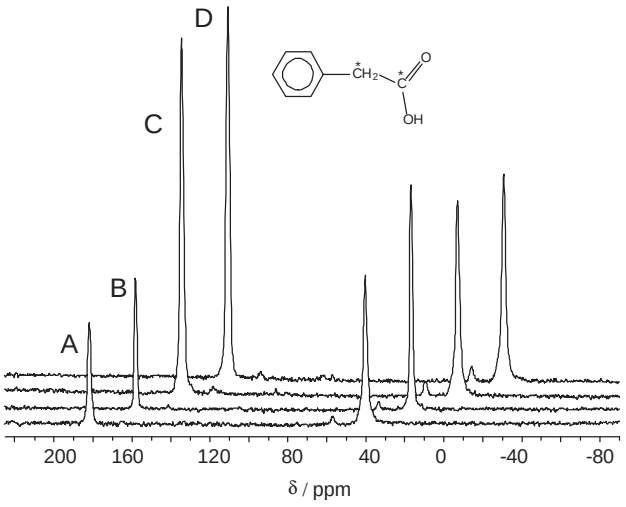

Figure 7: C-13 CP/MAS spectra of doubly-labelled (99%) phenylacetic-$^{13}C_2$ acid (B_0 = 9.4 T, ν_L = 100.6 MHz, ν_{rot} = 12576 Hz, number of acquisitions = 64, contact time = 3 ms). Spectrum 'A' was acquired using traditional Hartmann-Hahn CP and CW proton decoupling. Spectrum 'B' was acquired using Hartmann-Hahn CP and TPPM decoupling. Spectrum 'C' was acquired using VACP and CW decoupling. For spectrum 'D', the VACP and TPPM pulse programs were combined. Note that the carbonyl resonance benefits more from VACP while the methylene resonance benefits more from the TPPM decoupling. VACP provides a more intense peak due to a more efficient magnetization transfer from ^{1}H, while TPPM provides narrower lines with lower power ^{1}H decoupling.

trivial when the span of the chemical shift tensor is relatively small; spinning the sample rapidly will cause the sideband intensity to be concentrated in the isotropic peak. For cases where the chemical shift anisotropy is too large to be spun out, there are pulse sequences available to eliminate spinning sidebands. These include PASS (phase-altered spinning sidebands),[127] TOSS (total suppression of spinning sidebands),[128,129,130] TOSS-τ-reverse TOSS,[131] the four π pulse rotor-synchronized sequence of Geen *et al.*,[132] the five π pulse sequence of Song *et al.*,[133] SELTICS (sideband elimination by temporary interruption of the chemical shift),[134] and TIPSY (totally isotropic spectroscopy).[135] One technique which does not involve a special pulse sequence is VIABLE (variable-low-speed sideband suppression).[136] This technique is conceptually simple; it involves altering the MAS rate after the acquisition of each FID so that the sidebands do not become more intense as the number of acquisitions increases. Investigation of the theory, effectiveness, and limitations of some

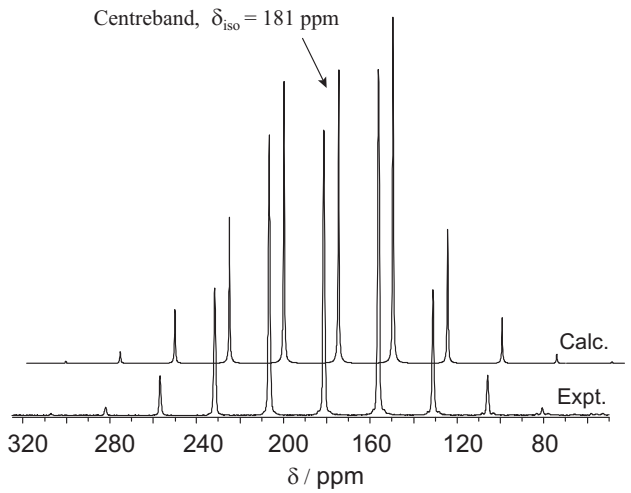

Figure 8: Experimental and simulated ^{13}C CP/MAS spectra of phenylacetic-*carboxy*-^{13}C acid (99% enriched). The experimental spectrum was acquired on a Bruker AMX spectrometer (B_0 = 9.4 T, $\nu_{\rm L}$ = 100.6 MHz), $\nu_{\rm rot}$ = 2530 Hz, number of acquisitions = 128. The Herzfeld-Berger analysis was carried out using the program "HBA"; the simulated spectrum was generated using the HBA parameters and the program "WSOLIDS". The simulated spectrum is offset along the horizontal axis to facilitate comparison with the experimental spectrum. Carbonyl carbon chemical shift principal components: δ_{11} = 258 ppm, δ_{22} = 176 ppm, δ_{33} = 110 ppm. The fine structure at the base of the peaks in the experimental spectrum is due to naturally-abundant phenyl carbons whose isotropic resonances are centred near 130 ppm.

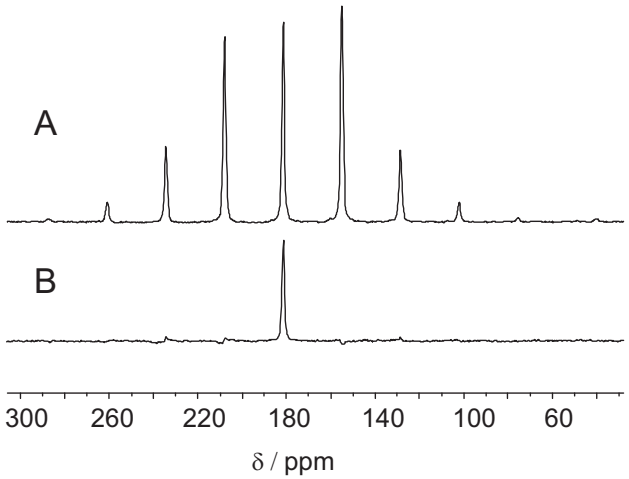

Figure 9: Carbon-13 CP/MAS spectra of singly-labelled (99%) phenylacetic-*carboxy*-^{13}C acid (B_0 = 4.7 T, $\nu_{\rm L}$ = 50.3 MHz, $\nu_{\rm rot}$ = 1.339 kHz) acquired with high-power proton decoupling. In spectrum A, a standard CP pulse program was used. The isotropic peak is at 181 ppm. In spectrum B, the TOSS sequence has been used to suppress the spinning sidebands; only the isotropic peak remains. One drawback of the TOSS sequence is the loss of intensity relative to the standard CP/MAS spectrum. Number of acquisitions: 64 (trace A); 128 (trace B).

of these techniques (primarily TOSS) may be found in the original literature.[133,137,138,139,140,141,142] Although there have been improvements made to the original TOSS experiment, the pulse program is widely available and the results it generates serve to illustrate the effect of sideband suppression. Shown in Figure 9 are ^{13}C CP/MAS spectra of singly-labelled (99%) phenylacetic-*carboxy*-^{13}C acid. The benefits of TOSS are evident in the lower trace, where the sidebands are nearly completely suppressed. The spinning-sideband-suppression techniques mentioned above would clearly be useful for identifying the isotropic peaks in a complicated CP/MAS spectrum with multiple sites with large chemical shift anisotropies.

3.2.3 High-Power Abundant Spin Decoupling

For solids, decoupling of abundant spins such as protons requires much more power than is generally required for solution samples. In the solid state, decoupling fields on the order of at least 60-100 kHz are required for ^{1}H decoupling. Typically, higher decoupling fields provide better signal-to-noise. As described in Section 2.2, the decoupler can only be switched on for a relatively short time (tens of milliseconds depending on the probe and the power levels), otherwise the rf coil will become very hot, leading to arcing and sample heating. Also, expensive capacitors may have to be replaced. It is especially important to pay attention to the conventions used in the spectrometer software. Depending on the software, the default units for the acquisition time may be seconds or milliseconds. It may be surprisingly easy to accidentally set the acquisition time to 50 s rather than 50 ms! Such errors will lead to expensive probe repairs and potentially to sample destruction.

Standard high-power proton decoupling in the solid state involves continuous wave (CW) decoupling. For ^{13}C CP/MAS experiments, the strongly dipolar-coupled CH_2 group of glycine provides a good test of decoupler efficiency. Fumaric acid monoethyl ester is also a useful sample since it contains methine, methylene, methyl, and carboxyl carbons. The effects of decoupling on line shapes in SSNMR have been discussed.[143,144,145,146] A recent paper by Van-

derHart and Campbell[90] provides an in-depth examination of the factors which influence the ^{13}C CP/MAS linewidth in solids for strongly ^{1}H-coupled carbon nuclei. A technique which provides improvements in both the resolution and sensitivity of the dilute-spin spectrum is known as two-pulse phase-modulated (TPPM) decoupling.[89] Briefly, this scheme involves a series of pulses of alternating phase, applied to the abundant-spin channel. The result is comparable to using higher CW decoupling fields. Experimentally, there is an additional pulse length and phase which must be optimized when using TPPM decoupling. Given the ease of using this pulse sequence and the excellent results it yields, it is recommended that TPPM decoupling be made standard for any dilute-spin solid-state NMR experiment; we have adopted this practice in our laboratory. In fact, a pulse program which combines both VACP and TPPM is extremely useful for CP/MAS experiments of dilute spins. Shown in Figure 7 are ^{13}C spectra of Ph^{13}CH$_2$^{13}COOH acquired under the following conditions: (A) standard CP/MAS, CW decoupling; (B) CP/MAS, TPPM decoupling; (C) VACP/MAS, CW decoupling; (D) VACP/MAS, TPPM decoupling. Clearly, the signal-to-noise ratio and linewidth benefit from VACP and TPPM. Stationary samples also benefit from TPPM decoupling (see Figure 3). It is apparent in Figure 3 that the use of TPPM is beneficial for resolving the features of the ^{13}C spectrum of a stationary sample of Ph^{13}CH$_2$^{13}COOH. Other frequency-modulated and phase-modulated decoupling sequences have also been developed.[91,147] It is important to note that in some cases, molecular dynamics may interfere with mechanisms used to narrow the spectra, e.g., ^{1}H decoupling; this may result in an unexpectedly broad resonance.[148]

3.2.4 Spectral Editing and Assigning Spectra

As mentioned above, the relative intensities of peaks in CP/MAS spectra are not necessarily related to the absolute number of nuclei resonating at a particular frequency. Several techniques have been developed to aid in the assignment of CP/MAS spectra. Recently the RAMP-CP method,[120] when used at high MAS rates, was shown to provide a ^{13}C spectrum of *N*-*t*-Boc-alanine with reliable relative intensities.[149] Spectral editing techniques may be used to separate resonances in a spectrum based on the chemical environments (typically the number of attached protons) of the various nuclei. For example, Emsley and co-workers have recently employed heteronuclear (^{13}C-^{1}H) indirect nuclear spin-spin couplings to discriminate between carbon atoms with differing numbers of directly-bonded protons.[150,151] Since the initial rate of CP defined by T_{IS} is based on the second moment[20,41] of the dipolar coupling between the dilute and abundant spins, in crystalline compounds it is possible to take advantage of the fact that, in the case of ^{13}C NMR for example, methylene and methine carbons should polarize faster than methyl and quaternary carbons; a short contact time should produce a spectrum consisting of only CH and CH_2 signals. Non-quaternary suppression (NQS), (also known as "dipolar dephasing" and "interrupted decoupling"), is a relatively straightforward technique which allows one to distinguish quaternary carbon atoms from those with one or two directly-bonded protons.[152] This discrimination is based on dipolar coupling between directly-bonded protons and the carbon atoms. The NQS pulse sequence uses a time period, or 'window', on the order of 40 μs before acquisition of the FID, when the proton decoupling is switched off. During this window, the signals due to methine and methylene carbon nuclei decay rapidly since they have shorter T_2s. Since methyl groups generally rotate rapidly in solids, averaging to a certain extent the ^{13}C-^{1}H dipolar interaction, signals from methyl carbons are usually not significantly suppressed during the 40 μs dephasing period. In fact, any group undergoing motional averaging of the dipolar interaction will give rise to unexpected intensity; this can be a first indication of dynamics. The simplification resulting from NQS is illustrated in Figure 10. Shown in the top trace is the ^{13}C CP/TPPM/MAS spectrum for a natural abundance powder sample of *p*-hydroxyacetanilide (Acetaminophen, Tylenol®). In the lower trace, the signal due to four of the aromatic ring carbons has been suppressed. Furthermore, dipolar splitting due to the ^{14}N nucleus is apparent in two signals; the high- and low-frequency signals are assigned to the carbonyl carbon and the *ipso* carbons, respectively. The signal due to the methyl carbon around 23 ppm is partially suppressed. Using special spectral editing techniques, it is possible to completely decompose a ^{13}C CP/MAS spectrum into four constituent spectra showing peaks from only quaternary or non-protonated carbons, methine carbons, methylene carbons, and methyl carbons.[153,154,155,156] Fumaric acid monoethyl ester is a useful setup sample for ^{13}CP/MAS spectral editing techniques. Recently, a technique known as SPECIFIC CP (spectrally induced filtering in combination with cross-polarization)[157] was developed; this method should prove to be very useful in spectral assignment and simplification in heteronuclear spin systems.

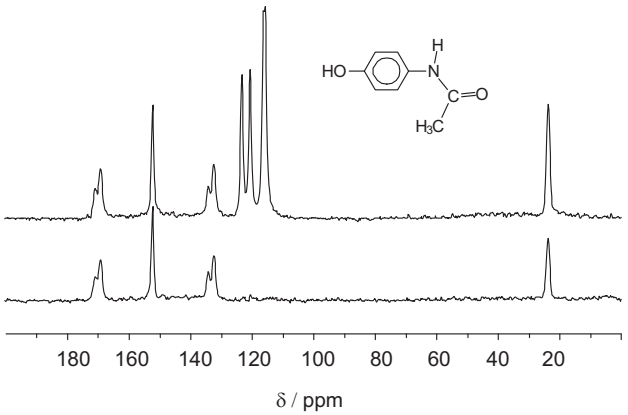

Figure 10: C-13 CP/MAS spectra with TPPM decoupling of *p*-hydroxyacetanilide (Acetaminophen, Tylenol®), B_0 = 4.7 T, $\nu_{\rm L}$ = 50.3 MHz, $\nu_{\rm rot}$ = 4780 Hz, number of acquisitions = 1024. In the bottom trace, non-quaternary suppression has been used to edit the spectrum. The signals due to the four protonated aromatic carbons are suppressed since they have directly bonded protons. The signals due to the carbon atoms directly bound to ^{14}N exhibit residual dipolar coupling. The methyl carbon resonance at about 24 ppm is not suppressed because the ^{13}C-^{1}H dipolar interaction is partially averaged as a result of rapid rotation about the local C_3 axis.

3.3 Some General Considerations: Shimming, Setting the Magic Angle, Referencing, Air Sensitive Samples, and Temperature Effects

Most of the considerations discussed in this section are equally applicable for SSNMR studies of quadrupolar nuclei. It is very important to pack the sample such that it is completely encompassed within the rf coil. Shimming a MAS probe has been discussed;[158] the ^{13}C CP/MAS signal of adamantane is useful since low decoupling power is required and line widths of 5-10 Hz or less are expected. MAS probes are designed such that the sample is held at approximately the magic angle; however, it is necessary to be able to adjust the angle. In addition, changing the spinning rate may cause small changes in the spinning angle.[159] One of the most common methods to adjust the magic angle is by observing the ^{79}Br ($I = \frac{3}{2}$) NMR spectrum of crystalline KBr.[160] In Figure 11, the ^{79}Br FIDs and NMR spectra of KBr are shown, both at the magic angle and off the angle. With experience, one should be able to adjust the magic angle from the FID. The FID shown in Figure 11a illustrates the rotational echoes arising from the $-\frac{3}{2}\leftrightarrow-\frac{1}{2}$ and $\frac{1}{2}\leftrightarrow\frac{3}{2}$ transitions with the transmitter set on the central transition centreband. Another commonly used magic angle calibration standard is the ^{23}Na ($I = \frac{3}{2}$) NMR of $NaNO_3$. The ^{23}Na NMR spectrum is shown in Figure 12, acquired with spinning at, or very near, the magic angle. Both ^{23}Na and ^{79}Br have resonance frequencies that are close to ^{13}C, so one may mix KBr or $NaNO_3$ with a ^{13}C setup sample, such as adamantane, in one rotor. It is easy to recognize when the magic angle is not adjusted correctly (Figure 11). Figure 13 illustrates the effect of changing the angle on the ^{13}C CP/MAS spectrum of hexamethylbenzene. In the off-angle spectra, the width of the peak arising from the aromatic carbons is scaled by $(3\cos^2\beta - 1)/2$ where β is the angle at which the sample is spinning relative to B_0. For this compound, the shape of the isotropic peak depends on whether the angle is greater than (Figure 13a) or less than (Figure 13b) the magic angle.

While KBr and $NaNO_3$ are convenient for ^{13}C CP/MAS NMR, using these calibration standards to set the magic angle for ^{31}P MAS NMR involves a significant retuning of the probe as well as other hardware modifications for some spectrometers. One compound suggested for setting the magic angle using ^{31}P NMR is zinc(II) bis(O,O'-diethyldithiophosphate), $Zn[S_2P(OC_2H_5)_2]_2$.[161] The two peaks in the ^{31}P CP NMR spectrum of a spinning sample become asymmetric with an offset from the magic angle of as little as 0.1°. Other candidates for setting the magic angle are tricyclohexylphosphine[162] and dimethylphenylphosphine oxide.[163] An additional accurate method for setting the magic angle is based on observing the NMR spectra of oriented molecules.[164,165] A standard has also been proposed for setting the magic angle for ^{19}F NMR experiments.[166]

For routine solid-state NMR work, it is convenient to have a solid sample which can be used to both set up the solid-state experiment (*i.e.*, the CP condition) as well as serve as a chemical shift reference. Over the years, a number of references have become commonly used among NMR spectroscopists. In the case of ^{199}Hg NMR, the accepted chemical shift reference, liquid dimethylmercury, is extremely toxic. Handling a solid reference compound is much safer. A list of references for spin-$\frac{1}{2}$ nuclei commonly studied in the solid state is given in Table 2.[105,167,168,169,170,171,172] Although twenty years old, Brevard and Granger's *Handbook of High Resolution Multinuclear NMR*[173] is an excellent source of useful high-resolution (solution) setup information for nuclei up to $Z = 83$ (bismuth). Harris' article in the *Encyclopedia of Nuclear Magnetic Reso-*

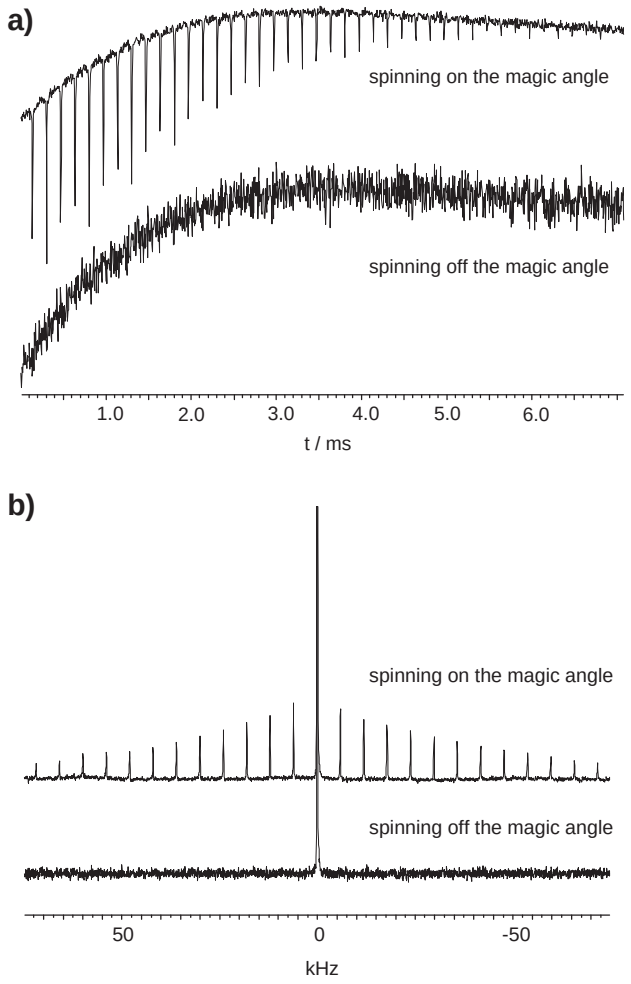

Figure 11: (a) The ^{79}Br NMR FID in polycrystalline KBr both on and off the magic angle and (b) the corresponding ^{79}Br MAS NMR spectra. The spinning frequency for both spectra is 6000 Hz. In both cases, 16 transients were acquired. $B_0 = 4.7$ T.

nance provides an authoritative summary of primary references and nuclear spin properties.[167]

It is common practice in solid-state NMR to use external references, which generally introduces an error in the chemical shift due to differences in the bulk susceptibility of the reference vs. the sample of interest.[174] In most cases, the correction is small and can be generally safely ignored. One exception is ^{1}H NMR, for which accurate chemical shift referencing requires special measures. In most cases, liquid external references (e.g., ethanol, TMS in deuterated solvents, etc.) are used to reference ^{1}H NMR spectra in the solid state. One group has used calcium hydroxyapatite, $Ca_5(OH)(PO_4)_3$, as a reference with the ^{1}H res-

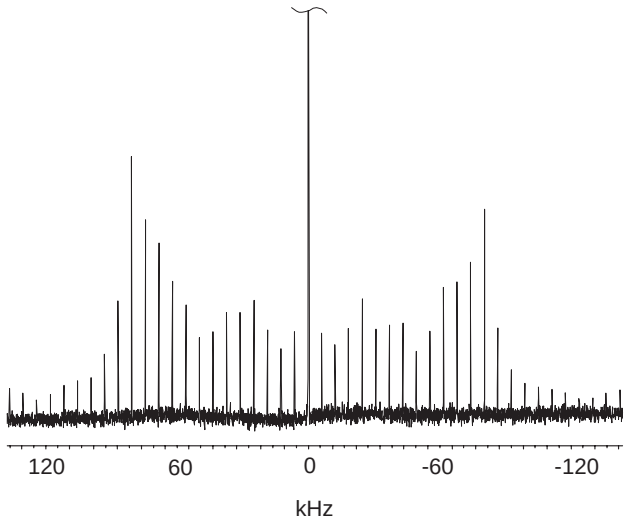

Figure 12: The ^{23}Na NMR spectrum of $NaNO_3$ acquired with sample spinning at the magic angle (spinning rate of 6012 Hz, 16 transients). $B_0 = 4.7$ T.

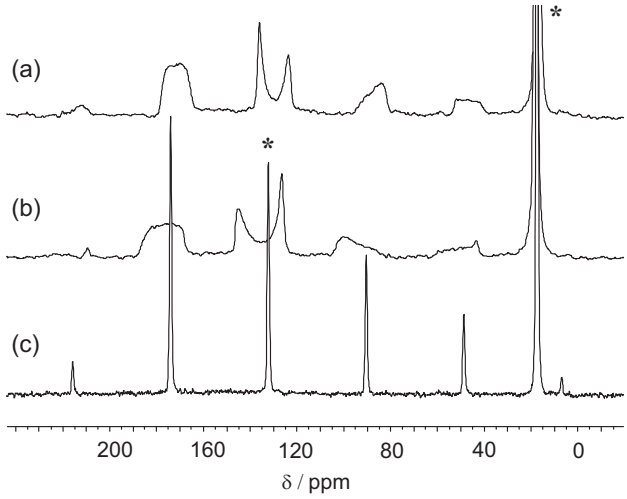

Figure 13: Carbon-13 CP NMR spectra of hexamethylbenzene, with $B_0 = 4.7$ T and the sample spinning at (a) greater than the magic angle and (b) less than the magic angle, and (c) at the magic angle. In all cases, 512 transients were acquired with the sample spinning at 2100 Hz. The isotropic peaks are marked with asterisks. The large peak on the right is due to the methyl carbons.

Table 2: Primary and Secondary Chemical Shift References for some Spin-$\frac{1}{2}$ Nuclei.

Nucleus	Primary Reference (167,173)	Secondary Reference (Solid)	δ_{iso} /ppm (relative to primary reference)
^{13}C	tetramethylsilane, $(CH_3)_4Si$ (neat liquid)	adamantane, $C_{10}H_{16}$	38.55, 29.50 (two peaks)(105,106b)
^{15}N	ammonia, $^{15}NH_3$ (neat liquid, 20°C)	ammonium nitrate, $^{15}NH_4NO_3$	23.45 (169); 23.80 (170)
^{19}F	fluorotrichloromethane, $CFCl_3$	liquid C_6F_6	-163.8 (171)
^{29}Si	tetramethylsilane, $(CH_3)_4Si$	sodium 3-(trimethylsilyl)-propane-1-sulfonate, $(CH_3)_3Si(CH_2)_3SO_3Na$	1.534 (peak has fine structure) (105b)
^{31}P	phosphoric acid, H_3PO_4 (85% in D_2O)	ammonium dihydrogen phosphate, $NH_4H_2PO_4$	0.81 (59)
^{77}Se	dimethyl selenide, $(CH_3)_2Se$	diammonium selenate, $(NH_4)_2SeO_4$	1040.2 (98)
^{113}Cd	cadmium perchlorate, $Cd(ClO_4)_2$ (1 M in water)[a)]	cadmium nitrate tetrahydrate, $Cd(NO_3)_2{\cdot}4H_2O$	-100.0 (102)
$^{117,119}Sn$	tetramethyltin, $(CH_3)_4Sn$	tetracyclohexyltin, $(C_6H_{11})_4Sn$	-97.35 (96, 99)
^{125}Te	dimethyl telluride, $(CH_3)_2Te$	telluric acid, $Te(OH)_6$	-692.2; -685.5 (two sites) (97)
^{195}Pt	$\Xi(^{195}Pt)$ = 21.496752 MHz[b)]	potassium hexa-hydroxyplatinate, $K_2Pt(OH)_6$	8024[b)] (99)
^{199}Hg	dimethylmercury, $(CH_3)_2Hg$ (neat liquid)	tetraethylammonium sodium tetracyanomercurate, $(NEt_4)Na[Hg(CN)_4]$	-434 (94)
		bis(tetrabutylammonium) tetrathiocyanomercurate(II), $(NBu_4)_2[Hg(SCN)_4]$	-615 (94)
^{207}Pb	tetramethyllead, $Pb(CH_3)_4$ or $\Xi(^{207}Pb)$ = 20.920597 MHz	$Pb(NO_3)_2$ (172)	[c)] (172)

[a)] Dimethylcadmium has also been suggested.[167] [b)] This is the Larmor frequency for ^{195}Pt when the proton frequency in TMS is exactly 100 MHz. Readers should be aware that some ^{195}Pt chemical shifts have been referenced to a value of 21.400000 MHz,[168] including the value of 8024 ppm given here. [c)] A comprehensive discussion of the pitfalls of ^{207}Pb chemical shift referencing is given in the literature.[172] This is required reading for proper referencing of lead chemical shifts.

onance of the hydroxyl group at 0.2±0.1 ppm from the protons in TMS.[175] In principle, spherical bulbs of reference material should be used for accurate chemical shift referencing.[23]

Samples which are air or moisture sensitive require some special precautions. Obviously, samples must be packed in a glove bag or glove box, depending on how sensitive the sample is. In general, the caps for most rotor designs are tight fitting and are sufficient for protecting moderately air sensitive samples for the duration of the experiment. For samples that are extremely air sensitive, various methods have been proposed,[176,177,178] e.g., sealed Pyrex or Kel-F MAS rotor inserts may be used.

The temperature effects of MAS mentioned briefly in Section 2.1.4 may be monitored by following the change in the chemical shift for nuclei such as ^{207}Pb in $Pb(NO_3)_2$,[179,180,181,182] ^{15}N in a tautomeric organic dye,[183,184] or ^{119}Sn in various stannates.[185,186] Temperature changes due to MAS are specific to the probe, manufacturer and operating conditions; hence, accurate variable temperature MAS work requires that one calibrates the sample temperature beforehand for the specific operating conditions being used.

3.4 Line Narrowing: Dealing with Abundant Spins (^{1}H and ^{19}F)

Nuclear magnetic resonance study of abundant spins (^{1}H and ^{19}F) in the solid state has been hampered by the large magnetogyric ratios (γ) and high natural abundance of these nuclei. It is thus somewhat disappointing that the very properties which make ^{1}H and ^{19}F NMR attractive in solution produce unique challenges for NMR investigations in the solid state. The large values of γ for both nuclei (26.7520×10^7 rad T^{-1} s^{-1} for ^{1}H and 25.181×10^7 rad T^{-1} s^{-1} for ^{19}F) result in large homonuclear direct dipolar coupling constants. An additional complication for ^{19}F is the possibility of large chemical shift anisotropy which can result in many ssbs under MAS conditions. The high natural abundance of both nuclei results in extensive dipolar couplings over a range of internuclear distances, often termed a "dipolar field", producing homogeneous and inhomogeneous broadening of the NMR spectrum. For example, single pulse excitation of ^{1}H in adipic acid, $HOOC(CH_2)_4COOH$, without magic-angle spinning of the sample produces a broad and featureless spectrum with a linewidth of about 15 kHz.[187] For comparison, the typical ^{1}H chemical shift range of organic molecules is approximately 15 ppm, corresponding to only 7.5 kHz for ^{1}H at 500 MHz (11.75 T). While MAS has been used to investigate ^{1}H NMR of solids,[175,188] the rate of sample spinning should be greater than the width of the spectrum. This may exceed the upper limit for many commercial MAS probes. Recently, ^{1}H NMR spectra obtained with very fast MAS (e.g., 35 kHz) have been published.[189,190] At these MAS rates, sample heating becomes a serious issue, in particular if one wishes to use this technique for low-melting materials or biological samples.

Detailed discussions of line narrowing techniques in solids have been presented elsewhere.[31,191,192] The two main strategies for line narrowing in solids are rapid rotation of the sample (*vide supra*) and manipulation of the spins via rf fields. For abundant spins, there are methods that combine sample rotation with spin irradiation, with each aspect designed to eliminate a particular line broadening mechanism, for example Combined Rotation And Multi-Pulse Spectroscopy (CRAMPS).[187,193,194] A less common method is zero-field NMR[195] where the sample is shuttled between the applied magnetic field and an area of very low applied magnetic field.[196] In CRAMPS, MAS at moderate speeds averages the chemical shift anisotropy and a special pulse sequence is used which effectively averages the homonuclear dipolar coupling. In the vector model, this is accomplished by rotating the magnetization with $\pi/2$ pulses along the x and y directions with phase cycling. The result is that the magnetization vector spends an equal amount of time along each of the *x, y* and *z* axes; hence, the time-averaged magnetization lies along the diagonal of the cube, which is oriented at the magic angle with respect to the applied magnetic field. The $(3 \cos^2 \theta - 1)/2$ factor that scales the dipolar interaction is thus zero; the pulse sequence produces the same result as MAS, but without the requirement for fast sample spinning. One basic four-pulse sequence which achieves this averaging is WAHUHA.[197] Other related pulse sequences, such as MREV-8[198] and BR-24[199] were developed to remove experimental artifacts associated with the WAHUHA sequence. These pulse sequences are usually included with the software of most commercial SSNMR spectrometers.

The pulse sequences used for CRAMPS are unusual in that the individual data points are detected between pulses in the sequence, rather than acquired after all the pulses have been applied. As an example, the WAHUHA sequence and the timing for data detection are illustrated in Figure 14. The experiment consists of the repetition of four $\pi/2$ pulses, with a data point acquired at time 0 and t_c, the cycle time (Figure 14). The acquisition point does not have to be in the mid-

dle of the observation window, as long as the interval between data collection is consistent. In setting up a CRAMPS experiment, the values used for t_c and the power for the $\pi/2$ pulses are critical. The cycle time needs to be significantly shorter than the rotor period and such that $t_c \ll \pi\ T_2$, *i.e.*, typically less than 40 μs.[194c] The $\pi/2$ pulse length needs to be much shorter than t_c, usually 2 μs or less. The pulses also have to be very homogeneous; hence the set up procedure for CRAMPS entails very careful tuning of spectrometer components. In addition, dedicated CRAMPS probes are also available.

It is important to note that these pulse sequences also affect the other interactions, such as the chemical shifts. In fact, the chemical shifts are scaled and the factor depends on the pulse sequence used. For WAHUHA, the scaling factor is $3^{-1/2}$.[194c] In general, however, this factor is determined for a given experiment and spectrometer by systematically incrementing the carrier frequency and observing the effect on the spectrum of a standard sample.

High-resolution ^{1}H NMR spectra of solids may also be acquired from samples where the protons are diluted with deuterons. This reduces strong ^{1}H-^{1}H dipolar coupling while MAS reduces the inhomogeneous ^{1}H-^{2}H dipolar coupling. Typically, the sample has to be 1% ^{1}H to obtain the best resolution;[200] deuterium decoupling is also necessary for optimal resolution. One can use samples at about 90% deuteration; however, high spinning speeds are required to achieve the same quality of spectra as one obtains with higher levels of deuteration and more modest spinning rates.[200] This method was first used to obtain high-resolution ^{1}H NMR spectra of organic compounds in the solid state[201] and later for some inorganic compounds.[202] Recently, the dipolar coupling between ^{1}H and ^{2}H was used to characterize the proton chemical shift tensor and hydrogen bonding in a series of ^{1}H dilute crystalline hydrates.[203] A review of some early work on ^{1}H solid-state NMR is provided in reference 192.

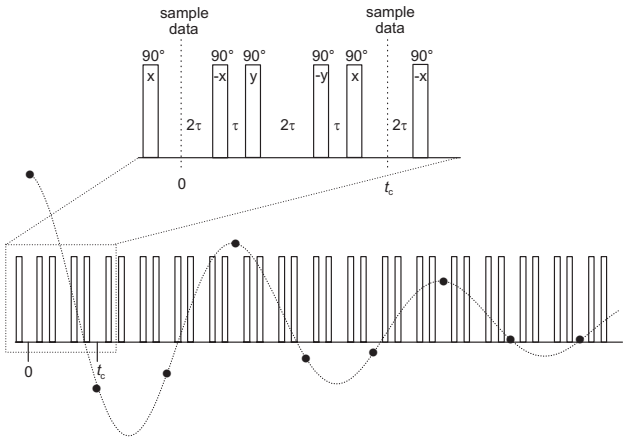

Figure 14: The WAHUHA pulse sequence for the CRAMPS experiment and the timing for data acquisition. The expanded region shows the details of the phase cycling and data sampling.

4 Non-Integer Quadrupolar Nuclei

4.1 The Quadrupolar Interaction

Smith and van Eck have recently reviewed the experimental advances in the solid-state NMR of half-integer quadrupolar nuclei.[204] Kentgens' practical guide to solid-state NMR of half-integer quadrupolar nuclei is highly recommended.[205] We will try to avoid extensive overlap with these reviews.

Nuclei with spin $I > \frac{1}{2}$ possess a nuclear quadrupole moment, eQ, because the nuclear charge distribution is non-spherical.[206] If the shape of the charge distribution is that of a prolate spheroid, eQ is positive; if it is oblate, eQ is negative. The nuclear quadrupole moment interacts with the electric field gradient (EFG) at the nucleus. The EFG is described by a symmetric, traceless second-rank tensor with five independent components, $V_{\alpha\beta}$. In its principal axis system, the EFG tensor is diagonal and can be characterized by two independent parameters: the largest principal component, $V_{ZZ} = eq_{ZZ} = \partial^2 V/\partial z^2$, and the asymmetry parameter, $\eta = (V_{XX} - V_{YY})/V_{ZZ}$, with the convention that $|V_{ZZ}| \geq |V_{YY}| \geq |V_{XX}|$. Laplace's equation for the electrostatic potential demands that $V_{XX} + V_{YY} + V_{ZZ} = 0$. The capitalized subscripts refer to the principal axis system of the EFG tensor. The product of the nuclear quadrupole moment and the largest component of the EFG tensor is known as the quadrupolar coupling constant, $C_Q = eQV_{ZZ}/h$. Some authors use the symbol χ to denote the quadrupolar coupling constant. Also, it is important to recognize that sometimes the quadrupolar coupling constant is expressed in radians s^{-1}, $eQV_{ZZ}/\hbar$.

In the absence of an external applied magnetic field, the axis of quantization for the quadrupolar nucleus depends upon the orientation of the EFG tensor at the nucleus. That is, the quadrupolar interaction ties the spin to the molecular framework since the EFG depends on the local environment of a nucleus. In the

presence of an external applied magnetic field, B_0, the Zeeman and quadrupolar interactions compete to determine the axis of quantization of the nuclear spin angular momentum. Pound first described quadrupolar effects on NMR spectra in crystals.[207,208] If the Zeeman interaction is much larger than the quadrupolar interaction (the high-field approximation), a number of simplifications result in treating quantum mechanical problems involving quadrupolar nuclei.

For a Zeeman interaction much larger than the quadrupolar interaction, one can show that, to first order, the transition frequencies are given by:

$$\nu_{m\leftrightarrow m-1} = \nu_0 - \nu_Q(2m-1)\times [3cos^2\theta - 1 + \eta sin^2\theta cos2\phi]/4 \quad (10)$$

where $\nu_Q = 3C_Q/[2I(2I-1)]$ and m ranges from I to (-I + 1). Expressions for the second-order quadrupolar Hamiltonian may be found in the original literature[209] or in review articles.[204,210,211,212] Note that when $m = \frac{1}{2}$, the central transition frequency, $\nu_{\frac{1}{2}\leftrightarrow-\frac{1}{2}}$, is simply equal to ν_0, to first order. Quadrupolar nuclei, in addition to being subject to the quadrupolar interaction, are also subject to the usual interactions experienced by spin-$\frac{1}{2}$ nuclei, such as dipolar coupling and anisotropic chemical shifts. Spectra of quadrupolar nuclei benefit from high-power proton decoupling as described in Section 3.2.3 for spin-$\frac{1}{2}$ nuclei. General considerations such as chemical shift referencing (Section 3.3) and setting the magic angle also apply to solid-state NMR studies of quadrupolar nuclei. Chemical shift references for some half-integer quadrupolar nuclei are given in Table 3.[213,214,215]

4.2 Setting the Pulse Width

In many cases, the central $\frac{1}{2} \leftrightarrow -\frac{1}{2}$ transition is of primary interest in the NMR of half-integer quadrupoles since the first-order quadrupolar interaction is zero; the satellite transitions extend over a wider spectral range, making them more difficult to observe. Single-pulse experiments on quadrupolar nuclei are referred to as broad line experiments.[210,216] As outlined by Abragam,[209] radiofrequency pulses on these nuclei may be classified as *selective* and *non-selective*. These terms refer to whether one or all of the allowed NMR transitions are excited. Equations 1 and 2 indicate the relationship between rf power, pulse width, and pulse length for a spin-$\frac{1}{2}$ nucleus. When the magnitude of the quadrupolar interaction is much less than the rf field strength, the equation $t_p = \pi/2\omega_{rf}$ is valid for maximizing the intensity for *non-selective* excitation of a quadrupolar nucleus. This corresponds to applying a "hard" pulse. In most non-cubic compounds it is not possible to satisfy the conditions for applying a strictly non-selective pulse.[210] When the quadrupolar interaction is much larger than the applied rf field, the optimum pulse widths for *selective* NMR excitation of any single-quantum transition for quadrupolar nuclei in the solid state are given by:[217]

$$t_p = \frac{\pi}{2\omega_{rf}\sqrt{I(I+1) - m(m+1)}} \quad (11)$$

For selective excitation of the central transition, equation 11 simplifies to dividing the solution $\pi/2$ pulse length by $(I + \frac{1}{2})$. For a powder sample, it is important to note that this does *not* mean that *only* the central transition is excited since, for certain orientations, the satellite transitions will be in the same spectral range as the central transition. Thus, for powder samples it is preferable to speak of "partly selective" pulses. In single crystals it may also be difficult, if not impossible, to apply perfectly "selective" or "non-selective" pulses.[218,219] The key practical consideration for acquiring spectra of powdered samples is that a shorter pulse will provide a more quantitatively reliable spectrum due to the relationship between pulse width and the spectral width which is excited (*vide supra*).[216] For example, using equation 11 and an rf field of 70 kHz on a spin-$\frac{3}{2}$ nucleus such as ^{23}Na or ^{11}B, we find that the pulse width should be 1.79 μs in order to "selectively" excite the central transition. Man *et al.* have compared the effects of $\pi/6$ vs $\pi/20$ pulses on ^{27}Al spectra of zeolite Y.[217] In addition to providing quantitatively reliable spectra, *i.e.*, accurate atomic site ratios, very short pulses are also required to ensure that the relative intensities of the discontinuities within a powder pattern for a single atomic site are accurate. In practice, to establish an appropriate pulse width, one may calibrate the $\pi/2$ pulse on a solution containing the nucleus of interest, *i.e.*, NaCl(aq) for ^{23}Na. Equation 11 may then be applied to determine the appropriate selective pulse width. For example, if we find that the $\pi/2$ pulse for ^{23}Na in NaCl(aq) is 2.1 μs, a selective pulse would be given by 2.1 μs / $\sqrt{4}$ = 1.05 μs ($I = \frac{3}{2}$; $m = -\frac{1}{2}$). In addition to carrying out one-pulse experiments, various quadrupolar spin-echoes are also commonly employed (*vide infra*).[210] For many of these experiments, $\pi/2$ and π pulses are used; thus knowledge of these parameters in addition to the selective pulse width is valuable.

Table 3: Primary and Secondary Chemical Shift References for Selected Half-Integer Spin Quadrupolar Nuclei.

Nucleus	Primary Reference (167,173)	Secondary Reference	δ_{iso} /ppm
^{7}Li	LiCl (1 M in H_2O)	LiCl (s) [a)]	-1.06 (213)
^{11}B	$F_3B{\cdot}O(C_2H_5)_2$ ($CDCl_3$ solution)	$NaBH_4$ (s)	-42.06 (105)
^{17}O	neat D_2O	[a)]	-
^{23}Na	NaCl (1 M in H_2O)	NaCl (s)	7.21 (105)
^{27}Al	$Al(NO_3)_3$ (aq)	$NaAlO_2$ (s)	79.33 (105)
$^{35/37}$Cl	NaCl (inf. dilute in H_2O)	NaCl (s)	-45.37
^{59}Co	$K_3[Co(CN)_6]$ (aq)	[a)]	-
^{63}Cu	$[Cu(CH_3CN)_4][ClO_4]$ (CH_3CN solution)	[a)]	-
^{95}Mo	Na_2MoO_4 (2 M in H_2O, pH = 11)	$Mo(CO)_6$ (s)	-1854 (214)
^{133}Cs	$CsNO_3$(aq), CsCl (aq)	CsCl (s)	223.2 (215)

[a)] Typically the primary reference has been used for referencing purposes.

4.3 CP to Quadrupolar Nuclei

Cross-polarization experiments involving quadrupolar nuclei are not yet "routine" in the sense that they are for many spin-$\frac{1}{2}$ nuclei such as ^{13}C, ^{15}N, and ^{31}P. Nevertheless, we provide some references here to recent theoretical and experimental work on cross-polarization involving half-integer quadrupolar spins. Some early experiments involved CP from protons to ^{23}Na,[220] ^{11}B,[221] ^{17}O,[222] ^{27}Al,[223] and ^{95}Mo.[224] The distorted lineshapes arising as a result of CP to half-integer quadrupolar nuclei have been discussed.[225,226] Subsequently, Frydman's development of the two-dimensional multiple-quantum MAS experiment[227] provided an impetus to examine ^{1}H→^{27}Al and ^{19}F→^{27}Al CP.[228] The groups of Wimperis and Grey have been particularly active recently in the study of CP involving quadrupolar nuclei;[229,230] Griffin has also contributed to this area.[231] CP/MAS experiments involving two quadrupolar nuclei, e.g., ^{27}Al→^{11}B have been discussed.[232,233] CP/MAS from a quadrupolar nucleus (e.g., ^{27}Al, ^{23}Na) to a spin-$\frac{1}{2}$ nucleus, ^{29}Si, has also been studied.[234] One of the key issues which complicates CP involving quadrupolar nuclei is the orientation dependence of the quadrupolar interaction. As a result of this dependence, only some of the spins in a powder can satisfy the Hartmann-Hahn condition for a given applied rf field strength. Thus, naive application of CP to quadrupolar nuclei will lead to distorted line shapes.

4.4 Stationary Samples

4.4.1 Broad-Line Experiments

Broad-line experiments on quadrupolar nuclei will yield a powder pattern resulting from contributions from all NMR interactions, *i.e.*, direct and indirect spin-spin coupling, anisotropic nuclear magnetic shielding, and the quadrupolar interaction. For most quadrupolar nuclei, the quadrupolar interaction will dominate the spectrum. If the quadrupolar parameters for a nucleus in a particular system are known, for example from an MAS experiment (*vide infra*), then under favourable conditions information about other interaction tensors such as the chemical shift tensor may be determined from the spectra of stationary samples. For quadrupolar nuclei in sites of tetrahedral or octahedral symmetry, typically the quadrupolar coupling constant is very small or zero.

A simulated powder pattern for a spin-$\frac{3}{2}$ nucleus (e.g., ^{11}B, ^{23}Na, ^{63}Cu, ^{87}Rb) with an axially symmetric EFG ($\eta = 0$), under stationary conditions, is shown in Figure 15. For nuclei with spin $\frac{n}{2}$, the first-order quadrupolar interaction does not influence the symmetric transitions, most importantly the central $\frac{1}{2} \leftrightarrow -\frac{1}{2}$ transition. For this reason, the central signal in Figure 15a appears as a symmetric, featureless peak. However, if the quadrupolar interaction is sufficiently strong (compared to the Zeeman interaction), the effect on the central transition of the second-order quadrupolar interaction may be observed and

simulated.[210] In practice, simulation of second-order effects are most often used to extract useful information from the spectrum. The effect of the second-order quadrupolar interaction, under stationary conditions, on the central transition of a spin-$\frac{3}{2}$ nucleus is shown in Figure 15b. Note the change in scale compared to Figure 15a. Thus, the effect of the second-order quadrupolar interaction is to change the original unperturbed symmetric peak into a signal with a distinct line shape. For isolated spins with an asymmetric EFG tensor, $\eta \neq 0$, simulated spectra are shown in Figure 16 and have been presented in the original literature.[235] and in review articles.[204,210,236] Granger has developed a simple method for determining C_Q, η, and the isotropic chemical shift from a spectrum of a stationary powdered sample.[237] This method does not provide any orientation information about the EFG and chemical shift tensors, but does provide the above mentioned parameters from a single spectrum without the aid of a computer simulation program.

Amoureux *et al.* have provided a careful summary of equations relating to the lineshapes of half-integer spin quadrupolar nuclei under stationary and MAS conditions.[238] For example, the full breadth of the central transition line shape, $\Delta\nu''_{TS}$, is given by:

$$\Delta\nu''_{TS} = \frac{(25+22\eta+\eta^2)}{144} \times \left[\frac{(3C_Q)^2}{((2I)(2I-1))^2}\right]\left[\frac{I(I+1)-\frac{3}{4}}{\nu_0}\right] \quad (12)$$

The data plotted in Figure 17 should provide the reader with a sense of what magnitude of quadrupolar coupling constant can be dealt with using standard FT techniques. Shown in this figure is a plot of the quadrupolar coupling constant versus the Larmor frequency for half-integer spins. The results presented in this plot assume an asymmetry parameter of zero and a generous line width, $\Delta\nu''_{TS}$, of 100 kHz.

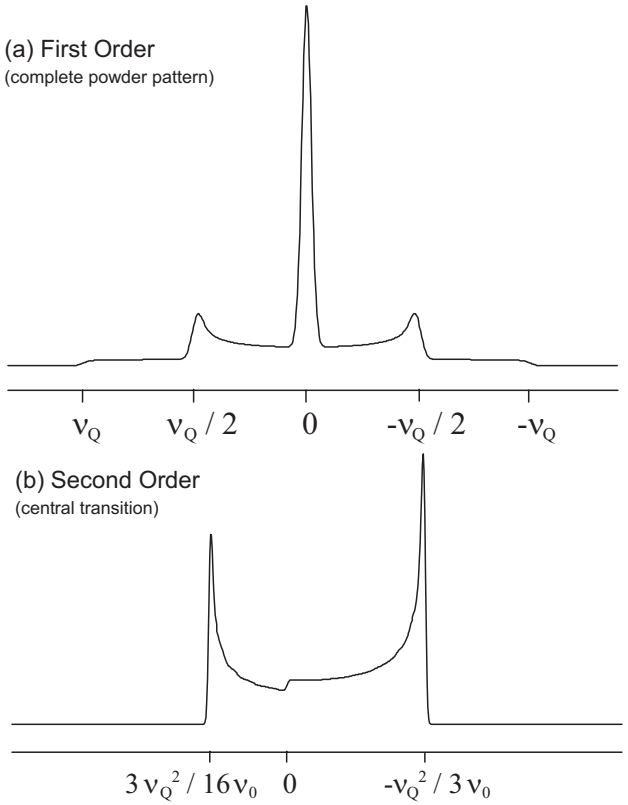

Figure 15: Simulated line shapes for a spin-$\frac{3}{2}$ quadrupolar nucleus under stationary conditions. In (a), signal arising from both the central $\frac{1}{2} \leftrightarrow -\frac{1}{2}$ transition and the satellite $\pm\frac{3}{2} \leftrightarrow \pm\frac{1}{2}$ transitions are shown. Only the first-order quadrupolar interaction is considered. In (b), the second-order quadrupolar line shape is shown for the central $\frac{1}{2} \leftrightarrow -\frac{1}{2}$ transition. Note the difference in scale between parts (a) and (b).

4.4.2 Quadrupolar Echo Experiments

Many quadrupolar nuclei of interest to scientists possess relatively low magnetogyric ratios, e.g., ^{25}Mg, $^{35/37}$Cl, $^{95/97}$Mo. For a given probe quality factor, Q, lower resonance frequencies lead to longer dead times which can corrupt the beginning of the FID. For particularly broad powder patterns this becomes especially important since most of the spectral information defining the line shape will be contained in the initial part of the FID. Probe ringing can also be a significant problem for low-γ nuclei. These problems may be overcome by the use of quadrupolar spin echoes.[239,240] Smith[241] has recently reviewed the progress in solid-state NMR of low-γ nuclei and provides an overview of some of the experimental approaches which are useful for dealing with low-γ nuclei, e.g., better probe design and spin echoes.

There are numerous variants of the original spin echo, $\pi/2$ - τ - π - τ - ACQ, depending on the nature of the spin system under study[20,210,239,242] (see also Section 5.1). The theory of quadrupolar spin-echoes in the presence of dipolar interactions has been discussed.[243,244] Chan has provided a lucid explanation of spin-echoes in half-integer quadrupole systems and discusses the terms "hard" and "soft" pulse in the context of density matrices and coherences.[239] A very useful recent paper by Bodart *et al.* provides a theoretical analysis and experimental investigation of

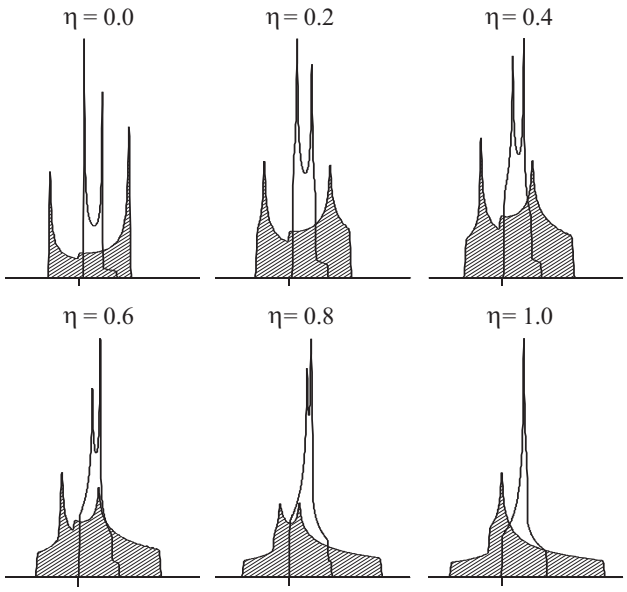

Figure 16: Simulated line shapes for the central $\frac{1}{2} \leftrightarrow -\frac{1}{2}$ transition of a half-integer quadrupolar nucleus. The broad, shaded spectra are for stationary samples and the narrower spectra are for MAS samples under the assumption of an infinite spinning rate. Both sets of spectra are shown as a function of the quadrupolar asymmetry parameter, η. The tick mark indicates the position of ν_0.

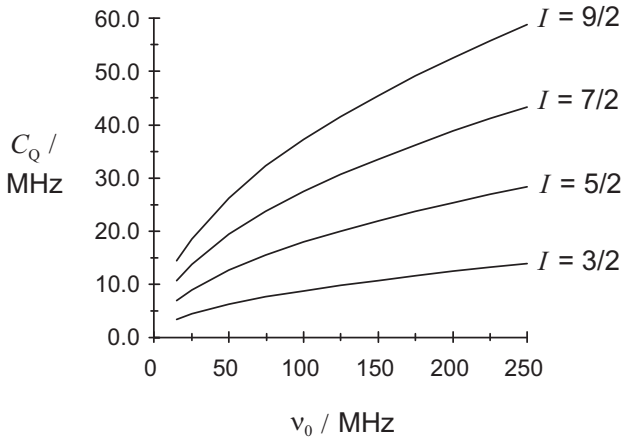

Figure 17: Plot of the quadrupolar coupling constant against the Larmor frequency of the quadrupolar nucleus for spins $I = \frac{3}{2}, \frac{5}{2}, \frac{7}{2}$, and $\frac{9}{2}$. For a stationary sample, the calculations are based on Equation 12 with the assumption of an axially symmetric EFG tensor and a central transition full line width of 100 kHz. The data may also be interpreted for MAS samples, where the only difference is that the assumed central transition full line width is 41 kHz.

quadrupolar echoes for half-integer spins in stationary samples.[245] They provide some general instructions for acquiring distortion-free spectra. The optimum rf field is determined to be $\Delta/(I + \frac{1}{2})$, where Δ denotes the static line width (in Hz) and I is the spin of the relevant nucleus, and irradiation must be performed at the centre-of-gravity of the line. The usual $\pi/2$ - τ - π - τ - ACQ sequence will give the maximum signal but does not minimize spectral distortions. To minimize the distortions, modifications must be made to pulse lengths and the optimum rf field strength must be reduced. The authors conclude that a $\pi/2$ - τ - $\pi/2$ - τ - ACQ sequence is a valid compromise. Phase cycling requirements as a function of spin number, $I = \frac{3}{2}, \frac{5}{2}, \frac{7}{2}, \frac{9}{2}$, are considered. It should be noted that while the work of Bodart *et al.* specifically discusses stationary samples, echoes can also be valuable in obtaining spectra of MAS samples.

The quadrupolar Carr-Purcell Meiboom-Gill[57] (QCPMG) echo experiment ("spikelet echo") has received considerable attention in the past few years[246,247,248,249,250,251] as a useful one-dimensional NMR probe of quadrupolar nuclei in stationary and MAS samples. This technique involves sampling the quadrupolar echo during a CPMG pulse sequence and can yield spectra with high signal-to-noise ratios when compared to a standard one-pulse or spin-echo experiment. The technique is therefore particularly useful for low-γ nuclei; some of the nuclei which have been studied using this technique include ^{87}Rb, ^{59}Co, ^{39}K, ^{25}Mg, ^{67}Zn, and ^{87}Sr.[247,250,251] Larsen *et al.* have employed the technique to determine the magnitudes and relative orientations of the chemical shift and EFG tensors for ^{87}Rb in $RbVO_3$ and ^{59}Co in $Co(NH_3)_5Cl_3$.[247]

It is important to recognize that an anisotropic chemical shift tensor will contribute to the spectrum of a quadrupolar nucleus in a stationary powdered sample.[215,252,253,254,255] Depending on the relative magnitudes of the chemical shift and EFG tensors, either effect could in principle dominate the observed spectrum. One must also be aware that the combined effect of chemical shift anisotropy and the anisotropic quadrupolar interaction does not necessarily lead to a broader powder pattern than that which would be observed in the absence of chemical shift anisotropy. This is due to the orientational dependence of both interactions. The relative orientations of the two interaction tensors, the span (Ω), and the skew (κ) of the chemical shift tensor are critically important to the appearance of the spectrum. Schurko *et al.* have provided an experimental example of a case where the effect of a non-zero span of the chemical shift tensor

decreases the breadth of the pure quadrupolar ^{27}Al powder pattern for $Cl_3Al{\cdot}OPCl_3$.[256]

4.5 MAS Powdered Samples

Standard MAS experiments on spin-$\frac{n}{2}$ quadrupolar nuclei result in narrowing of the central transition; typically the peak width is reduced by a factor of 3 to 4.[257,258] Calculated spectra of the central transition obtained with and without MAS, broadened by the second-order quadrupolar interaction, are shown in Figure 16 as a function of the asymmetry parameter. General equations which describe how the apparent isotropic chemical shift is modified by the second-order quadrupolar interaction under conditions of MAS have been given.[259,260] For example, in the case of a spin-$\frac{3}{2}$ nucleus, the centre of gravity of the central transition centreband (MAS or static) is displaced from the true isotropic resonance frequency by:

$$\Delta\nu_{+\frac{1}{2},-\frac{1}{2}} = -\frac{1}{40}\left(\frac{C_{\mathrm{Q}}^2}{\nu_{\mathrm{L}}}\right)\left(1+\frac{\eta^2}{3}\right) \qquad (13)$$

In addition, the position of the $\pm\frac{3}{2} \leftrightarrow \pm\frac{1}{2}$ satellite transition centrebands with respect to the central transition centreband is given by:[259]

$$\Delta\nu_{\pm\frac{3}{2},\pm\frac{1}{2}} - \Delta\nu_{+\frac{1}{2},-\frac{1}{2}} = \frac{3}{40}\left(\frac{C_{\mathrm{Q}}^2}{\nu_{\mathrm{L}}}\right)\left(1+\frac{\eta^2}{3}\right) \qquad (14)$$

Direct interpretation of MAS spectra of quadrupolar nuclei in terms of the line shapes is most straightforward when there is only one unique site. Of course, for many systems of interest, there exists more than one site. The ^{11}B MAS spectra of borax obtained at two different applied magnetic fields are shown in Figure 18. In borax, there are two unique boron sites. At the lower applied magnetic field strength (4.7 T), resolution of the signals in the spectrum is not achieved, and this complicates direct interpretation of the spectrum. At 17.63 T, however, the NMR signals from the two boron sites are clearly resolved and their respective line shapes are easily interpreted. One set of boron atoms are trigonally coordinated and, as a result of the significant boron quadrupolar coupling constant, give rise to a second-order powder pattern in the MAS spectrum. The other set of boron atoms are tetra-coordinate and, because of their high-symmetry environment, exhibit a very small quadrupolar coupling constant, such that no second-order quadrupolar splitting is observable even at low magnetic field strengths.

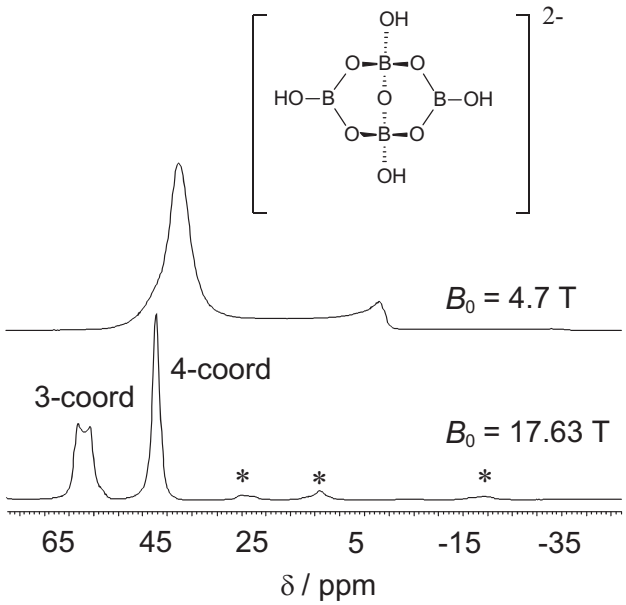

Figure 18: Experimental ^{11}B MAS NMR spectra of solid powdered sodium tetraborate tetrahydrate (borax) acquired at 4.7 T ($\nu_{\mathrm{L}} = 64.2$ MHz) and 17.63 T ($\nu_{\mathrm{L}} = 240.56$ MHz). The boron-containing anion has two distinct boron sites. Spinning sidebands are indicated by asterisks.

As a guide to what magnitude quadrupolar coupling constants may be observed for a given spin and Larmor frequency, the data presented for stationary samples in Figure 17 are also valid for MAS samples, where we have assumed zero asymmetry of the EFG tensor and a line shape of breadth 41 kHz (scaled by 2.43 relative to the stationary case). The use of higher applied magnetic field strengths to resolve individual sites in the MAS NMR of half-integer quadrupolar nuclei is not always feasible or sufficient when there are many different sites and when quadrupolar coupling constants are very large, especially for spin-$\frac{3}{2}$ and spin-$\frac{5}{2}$ nuclei. There are also many systems, e.g., glasses, where a distribution of quadrupolar parameters and chemical shifts exists due to the amorphous nature of the sample. As a result, several techniques beyond conventional one-pulse MAS or spin-echo MAS experiments have been developed. For example, variable-angle spinning (VAS) can be effective in reducing the width of the central transition in situations where second-order quadrupolar broadening is of significant magnitude.[261,262] Other variations on the standard one-dimensional MAS experiment for observing quadrupolar nuclei will be discussed briefly below.

Shown in Figure 19 are the relative integrated intensities and line widths for the allowed transitions of a

spin-$\frac{7}{2}$ nucleus, assuming an infinite MAS rate (derived from reference 259). The intensities are combined for each pair of satellites into their common central MAS line. It is interesting to note that the central transition is neither the most intense nor the narrowest. Satellite transition spectroscopy (SATRAS) experiments take advantage of two aspects of the MAS spectrum of a half-integer quadrupolar nucleus which are typically ignored in simple one-pulse experiments where the centreband of the symmetric central $\frac{1}{2} \leftrightarrow -\frac{1}{2}$ transition is interpreted.[257,263] In SATRAS experiments, one interprets the spinning sideband patterns arising due to the satellite transitions, *i.e.*, $\frac{3}{2} \leftrightarrow \frac{1}{2}, -\frac{1}{2} \leftrightarrow -\frac{3}{2}$ for a spin-$\frac{3}{2}$ nucleus. Jäger has written an excellent review which is recommended to anyone interested in performing SATRAS experiments.[264] Extremely stable fast MAS is essential to the success of these experiments. Excellent probe tuning is also critical for obtaining high-quality SATRAS spectra. Aside from these requirements, the actual experimental procedure for acquiring a SATRAS spectrum does not differ much from that used in a standard one-pulse experiment. An experimental ^{59}Co SATRAS spectrum of crystalline powdered Co(acac)$_3$ is shown in Figure 20. The inset shows some of the spinning sidebands arising from the satellite transitions for this spin-$\frac{7}{2}$ nucleus. SATRAS experiments are useful for the resolution of magnetically non-equivalent sites. For example, Power has used the technique to resolve three distinct sodium sites in crystalline sodium sulfite.[265] Other selected references are given where SATRAS methodology has been applied to ^{11}B[266] and ^{27}Al;[267] many of the systems studied are glasses.

Simulations of the effects of the second-order quadrupolar interaction are extremely useful in characterizing the EFG tensor for a quadrupolar nucleus in a given compound. However, in many situations it may be desirable to achieve even more "isotropic-like" spectra of spin-$\frac{n}{2}$ quadrupolar nuclei. For example, when many magnetically or crystallographically non-equivalent sites give rise to peaks in the spectrum, the result may be a broad, complicated peak which is difficult if not impossible to analyze. Within the last dozen years or so, three techniques have been developed to average the second-order quadrupolar interaction: double rotation (DOR),[268] dynamic angle spinning (DAS),[269] and multiple quantum MAS (MQMAS).[227] MQMAS was developed most recently, and since no special probes or other hardware are required for its implementation, this technique has become the most popular for obtaining high-resolution spectra of spin-$\frac{n}{2}$ quadrupolar nuclei. Applications of

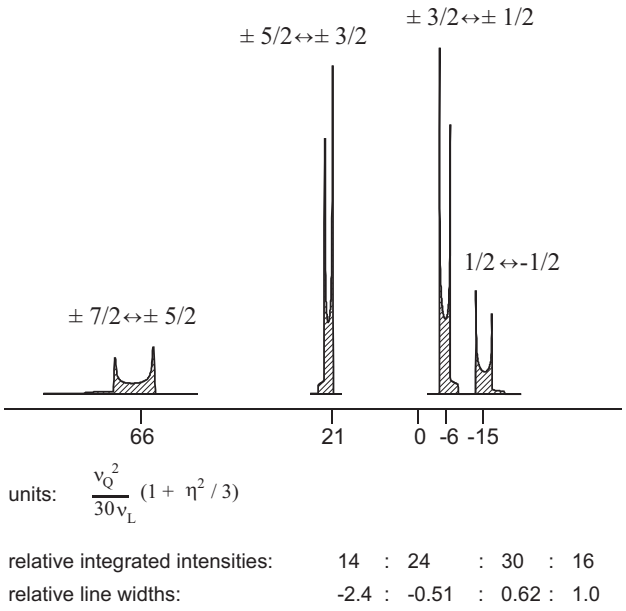

Figure 19: Simulated spectra for a spin-$\frac{7}{2}$ nucleus, assuming an infinite spinning rate where the intensity from all sidebands is concentrated in the centrebands for each transition. The intensities are combined for each pair of satellites into their common central MAS line.

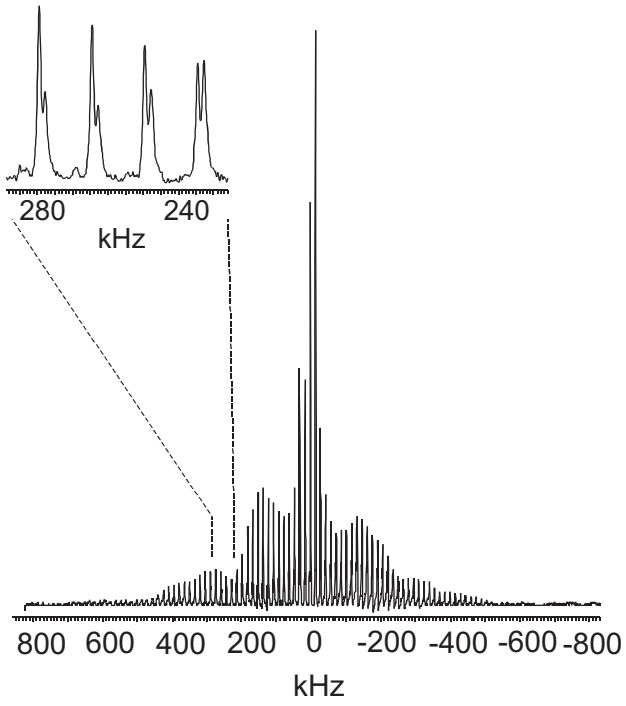

Figure 20: Co-59 SATRAS spectrum of solid powdered Co(acac)$_3$. Inset shows some of the satellite transition sidebands in detail.

SSNMR of quadrupolar nuclei in biological systems (e.g., ^{17}O, ^{67}Zn, ^{59}Co, ^{23}Na, ^{39}K), with an emphasis on MQMAS, have been reviewed by Wu.[270] MQMAS is a two-dimensional experiment and will not be discussed in this review. Most applications of DAS are also in a two-dimensional mode. Chmelka and Zwanziger's excellent review on theoretical and experimental aspects of both DOR and DAS is recommended reading for anyone interested in these experiments.[271] We provide here briefly the basic ideas behind the DOR and DAS experiments. These experiments achieve the goal of averaging second-order quadrupolar effects by averaging both the second- and fourth-order Legendre polynomials to zero: $\langle P_2 \rangle = \langle P_4 \rangle = 0$. This is done in two different manners, although both methods rely on mechanical movement of the rotor which differs from simple MAS. Because P_2 and P_4 have a different angular dependence, no single spinner axis angle can average them to zero simultaneously. In DOR, two rotors are used, one inside the other. The smaller inner rotor which contains the powdered sample spins at an angle of 30.56° with respect to a larger outer rotor. The larger rotor spins at the magic angle with respect to the external applied magnetic field. The resulting spectrum consists of relatively sharp symmetric peaks for each distinct resonance, flanked by a set of sidebands.[272] One of the main limitations on DOR is the maximum achievable spinning rate of the outer rotor ($\approx$ 1250 Hz);[205] this in turn limits the feasibility of the experiment for averaging highly anisotropic quadrupolar interactions. In DAS, the orientation of the rotor axis becomes a time-dependent part of the NMR experiment. By changing the rotor axis during the experiment, the anisotropic contributions to the spectrum are made to appear isotropic. The main limitation of DAS is that the T_1 of the quadrupolar nuclei must be sufficiently long with respect to the rotor flip time. Thus, the common key requirement of DAS and DOR is the need for additional hardware to perform the experiments.

4.6 Single-Crystal Studies

Single-crystal NMR studies on quadrupolar nuclei are essentially identical to the analogous experiments described in Section 3.1.2 for spin-$\frac{1}{2}$ nuclei, except that the dominant anisotropic interaction is usually the quadrupolar interaction. We refer the reader to Section 3.1.2 for the basic details of the single-crystal experiment and once again make mention of the excellent instructive papers of Kennedy and Ellis.[71] We also provide some recent references to single-crystal NMR studies of quadrupolar nuclei: the group of Jakobsen has studied ^{95}Mo in molybdenum hexacarbonyl,[273] ^{87}Rb in $RbVO_3$[274] and Rb_2CrO_4,[275] ^{69}Ga and ^{71}Ga in β-Ga_2O_3,[276] ^{27}Al in the garnet $Y_3Al_5O_{12}$[277] and ^{67}Zn in zinc acetate dihydrate;[278] the group of Wasylishen has studied ^{59}Co in $Co(acac)_3$[218] and ^{133}Cs in Cs_2CrO_4[279] and $CsCd(SCN)_3$;[72] Woo has carried out a ^{27}Al study of corundum;[280] Power *et al.* have studied a single crystal of vitamin B-12 *via* ^{59}Co NMR.[281]

5 Deuterium NMR: A Powerful Technique for Probing Molecular Dynamics

Several NMR methods have been developed to study molecular motion in solid materials. Here, we focus on ^{2}H NMR, which is a particularly powerful technique that has found widespread use in the investigation of molecular dynamics in organic molecules (e.g., polymers, model membrane systems).[88] The deuterium ($I = 1$) quadrupole interaction is sufficiently small to allow acquisition of undistorted ^{2}H NMR spectra and yet is large enough to be a sensitive probe of molecular dynamics.[282] Spin-lattice relaxation times are also extremely useful in characterizing rotational motion. For these reasons, and because the synthesis of compounds with deuterium labels at specific sites is relatively straightforward,[283] ^{2}H NMR is a popular method of investigating molecular dynamics. The theory underlying ^{2}H NMR has been outlined in several articles.[284] Also, the text of Schmidt-Rohr and Spiess[88] is highly recommended, particularly for a discussion of modern 2D ^{2}H NMR techniques.

5.1 Experimental Considerations

The ^{2}H NMR spectra of stationary powder samples, which have a spectral width that can exceed 300 kHz, present some unique challenges to the NMR spectroscopist, as discussed for spin-$\frac{n}{2}$ nuclei in Section 4. Since much of the information derived from such studies are based on line-shape analysis, uniform excitation of the complete spectrum is very important. This can be difficult using rf pulses of finite power.[285] The use of small coils (5 mm diameter or less) allows $\pi/2$ excitation pulses of approximately 2 μs, corresponding to an rf field of 125 kHz, which is in many cases comparable to the quadrupolar interaction. Composite pulse sequences have been proposed to uniformly excite the sample.[286] Other pulse sequences have also been pro-

posed,[287] but these sequences also produce distortions in the spectra.

As for spin-$\frac{n}{2}$ nuclei (*vide supra*), rapid free induction decay leads to difficulties. Quadrupolar echo pulse sequences, which refocus the signal after a suitable delay to allow probe recovery, have been developed to rectify this problem,[285,288] e.g., $(\pi/2)_x$ - τ_1 - $(\pi/2)_y$ - τ_2 - ACQ. The delays may be set such that acquisition begins at the echo maximum. In practice the delays are set such that $\tau_1 = \tau_2 + t$ where $t = 3$ to 10 μs, allowing the observation of the full echo. Before Fourier transformation, the FID must be left-shifted such that the echo maximum is the first point of the FID. The effect on the line shape of processing an FID for which the first point is not an echo maximum can be simulated (Figure 21) by left-shifting an FID by different amounts before processing. The lower trace, which is distorted significantly, corresponds to a spectrum processed such that the first point of the FID is 2.2 μs before the echo maximum. It is possible by a trial-and-error process to set the delays such that there is a point at the echo maximum, but such a procedure may be time-consuming. If the sampling rate is maximized by setting the dwell time to the lowest value allowed by the digitizer, there usually are sufficient points near the echo maximum to make distortions negligible. For example, the sampling rate would have to be at least ten times slower (dwell of 2 μs instead of 0.2 μs) to produce the distortion simulated in the lower trace of Figure 21. Fractional left-shifting[289] or interleaving[290] may also be used to ensure that there is a point at the echo maximum. Note that τ_2 as illustrated here is the total time after the second pulse and includes existing delays, such as the dead time. The total delay after the $\pi/2$ pulse must be sufficiently long to avoid problems from pulse breakthrough, as determined by examination of the start of the FID.

If the transmitter is centred exactly on the Larmor frequency, the receiver phase may be set such that all the signal intensity occurs in the real channel. This will give a spectrum with reflection symmetry about the Larmor frequency.[285] A $2^{1/2}$ enhancement in the signal-to-noise ratio may then be achieved by setting the value of all imaginary points of the FID to zero, but this should only be done after ascertaining that the spectrum is actually symmetric.[285] Magnetic shielding anisotropy, particularly at high field and/or in the presence of paramagnetic species, may cause asymmetry in the line shape.[291]

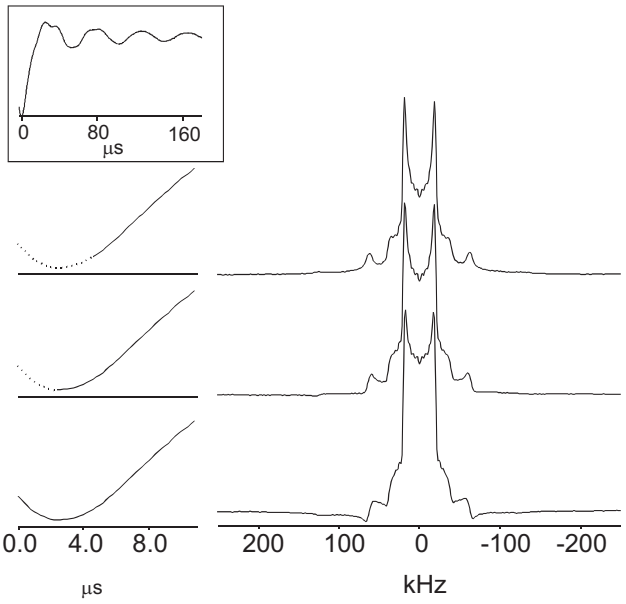

Figure 21: Deuterium NMR spectra of perdeuterated poly(methyl methacrylate) acquired at 9.4 T (right). The first 10 μs of the corresponding FIDs are shown at left. The solid line of the FID indicates the portion of the FID remaining after left-shifting (see text). All other processing parameters were the same. The complete FID is shown in the inset.

5.2 Deuterium NMR Spectra

In the absence of dipolar or indirect spin-spin coupling interactions, the contribution to the solid-state ^{2}H NMR spectrum of a single deuteron consists of two transitions. The separation between these transitions depends on the magnitude of the quadrupolar coupling constant, C_Q, and on the orientation of the principal axis system (PAS) of the EFG tensor relative to B_0.[284] Analysis of single crystals is possible if suitable crystals can be grown,[292,293,294,295] (*vide supra*) but it is more common to measure ^{2}H NMR spectra of powder samples. The random orientation of crystallites in such samples gives rise to the characteristic Pake doublet (Figure 22), a consequence of the two transitions (dotted lines). In this hypothetical spectrum, the EFG tensor is axially symmetric ($\eta = 0$) and there is only one ^{2}H site. Figure 23 illustrates how the ^{2}H powder line shape depends on η, all other parameters being the same. Values of C_Q and η may be derived from the discontinuities and shoulders in these spectra, denoted $\Delta\nu_i$ (Figure 23), according to:[296]

$$\Delta\nu_1 = \frac{3}{4}C_Q(1-\eta)$$

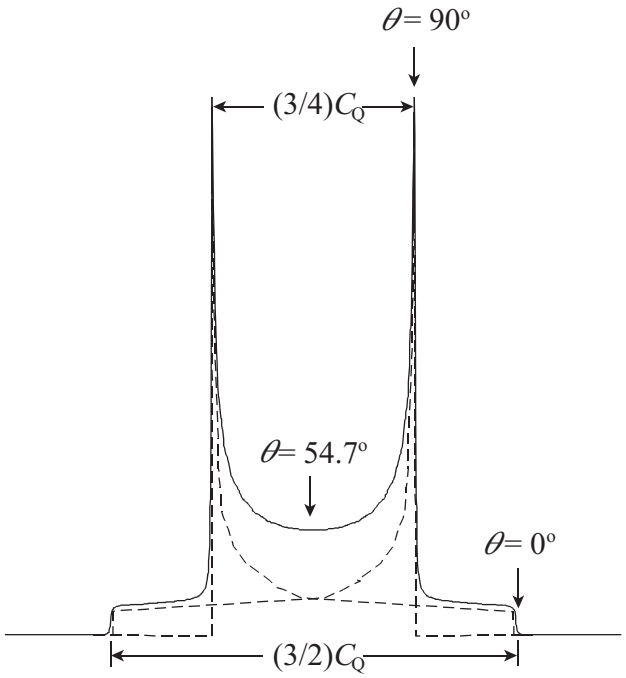

Figure 22: The Pake doublet, a typical ^{2}H NMR spectrum in the absence of any significant asymmetry in the EFG or anisotropy in the chemical shielding. Note that the orientation labelled 90° also contains a contribution to the total intensity from the other transition, corresponding to $\theta = 35.3°$, where θ defines the orientation of the largest component of the EFG relative to B_0.

$$\Delta\nu_2 = \frac{3}{4}C_{\rm Q}(1+\eta) \qquad (15)$$
$$\Delta\nu_3 = \frac{3}{2}C_{\rm Q}$$

These equations are valid *if motion is negligible*. More complex spectra result if motion is significant; the underlying theory for these more complex spectra have been discussed by Haeberlen[29] and Spiess.[297] Figure 24 illustrates the calculated and experimental spectra of perdeuterated poly(methyl methacrylate), pmma. Although $C_{\rm Q}$ for the CD_2 group is comparable to that for the CD_3 groups, the rapid rotation of the latter results in motional averaging of $C_{\rm Q}$; hence the contribution to the spectrum from these groups is scaled by a factor of (3 $\cos^2\beta$ - 1)/2, where β is the angle between the C-D bond and the axis of rotation ($\approx 109.47°$). The complete spectrum is the sum of the contributions from the individual sites.

Resolving ^{2}H sites with different chemical shifts can be very difficult, a consequence of the broad spectra of stationary powder samples and of the small chem-

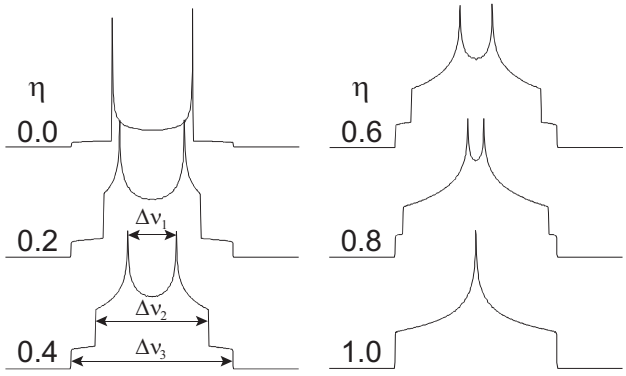

Figure 23: Dependence of the lineshape of a ^{2}H NMR spectrum of a stationary sample on the asymmetry in the EFG tensor, η. See text for a discussion of the discontinuities shown in the spectrum with $\eta = 0.4$.

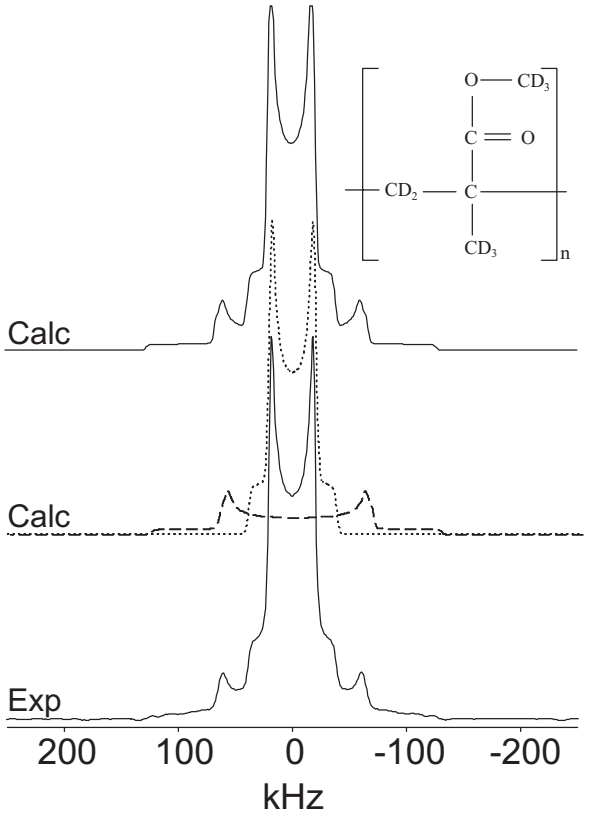

Figure 24: Deuterium NMR spectrum of a stationary sample of perdeuterated poly(methyl methacrylate) acquired at 4.7 T using the quadrupolar echo pulse sequence ($\pi/2$ = 2 μs, τ_1 = 25 μs, τ_2 = 20 μs). The middle trace is the calculated spectrum: contribution from CD_2 (– – –), $C_{\rm Q}$ = 165 kHz, η = 0.0; from CD_3 (· · · · · · ·), $\langle C_{\rm Q}\rangle$ = 52 kHz, η = 0.075; and the total calculated spectrum (upper trace). The experimental spectrum, (lower trace) was acquired by coadding 5648 transients.

ical shift range of ^{2}H. Yet the resolution of distinct deuteron sites is often an important component of a complete analysis. In many cases, the broadening arising from both the chemical shielding anisotropy and the first-order quadrupolar interaction may be removed by MAS.[125] For deuterium, the line-narrowing resulting from MAS is several orders of magnitude; hence, deuterons with chemical shift differences of less than 2 ppm may be resolved by this technique.[298,299] As with any quadrupolar nucleus (*vide supra*), the second-order quadrupolar interaction, which has a different angular dependence,[257] is not averaged by MAS. This has two consequences for ^{2}H NMR: a shift to low frequency[257] and a slight broadening[298a] of the isotropic peak. This amounts to a quadrupolar shift, $\delta^{(2)} = 2\nu_Q^2/(5\nu_0)$, of approximately 1 ppm at 4.7 T. The line broadening is approximately $\nu_Q^2/(12\nu_0)$, corresponding to about 20 Hz at 4.7 T. Here, ν_Q, $3C_Q/2$, is the quadrupole frequency. Since ν_Q is independent of B_0 while ν_0 is proportional to B_0, the line broadening and quadrupolar shift resulting from the second-order quadrupolar effect are negligible at higher fields. Numerous other line broadening mechanisms contribute to the observed linewidth; these have been discussed in detail elsewhere.[300] Figure 25 illustrates that the aliphatic and aromatic ^{2}H peaks are clearly resolved in the NMR spectrum of a MAS sample of acenaphthene-d_{10}. However, the chemical shift differences between individual aromatic ^{2}H sites are not resolved, a consequence of the almost equal chemical shifts of all aromatic deuterons in this sample.[301] This diagram also illustrates how the envelope of the spinning sideband pattern is similar to the spectrum of the stationary sample, shown in the upper trace. To minimize distortion of the spectra, shorter excitation pulses were used (1 μs, compared to a $\pi/2$ pulse of 2 μs). The ^{2}H NMR line shapes of MAS samples are very sensitive to the setting of the spinning angle. Deviations of a few hundredths of a degree can lead to hundreds of Hz of broadening of the peaks, obscuring most chemical shift differences.[298a] Double quantum techniques[302] and 2D experiments, which are less sensitive to the setting of the angle, have been proposed.[303]

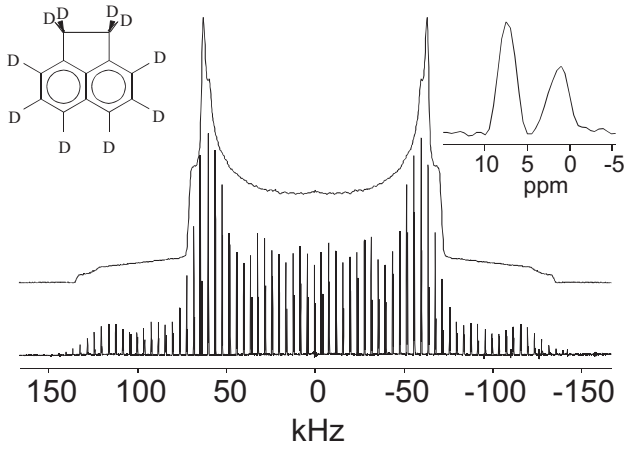

Figure 25: Deuterium NMR spectrum of a stationary sample of acenaphthene-d_{10} (upper trace) at 9.4 T acquired using the quadrupolar echo pulse sequence (τ_1 = 17 μs, τ_2 = 9 μs, $\pi/2$ = 2.3 μs). The lower trace illustrates the MAS ^{2}H NMR spectrum of this sample at ν_{rot} = 4 kHz and B_0 = 9.4 T. A single pulse sequence, with a 1.0 μs excitation pulse, corresponding to approximately $\pi/4$, was used. The expanded region illustrates the isotropic peaks; the separation between the peaks is approximately 6 ppm.

5.3 H-2 NMR Relaxation Times and Molecular Dynamics

In principle, one should consider five independent relaxation times when investigating the relaxation of $I =$ 1 nuclei,[304] three spin-spin and two spin-lattice relaxation times.[305] The latter are T_{1Z}, associated with the return of Zeeman energy to its equilibrium value, and T_{1Q}, related to the decay of the quadrupolar energy. The measurement of these relaxation times has been discussed in the literature.[304,305] The measurements of T_{1Z} and the ratio T_{1Z}/T_{1Q} are particularly useful since they are very sensitive to molecular motion.[282,306] The most reliable technique for measuring the spin-lattice relaxation time, T_{1Z}, is the inversion recovery pulse sequence.[41] In the case of ^{2}H, one monitors the echo intensity after inserting the delays and the $(\pi/2)_y$ pulse as for the standard quadrupole echo experiment. A 16-step phase cycle is recommended to suppress single and double quantum artifacts.[292] The pulse sequence used to acquire the spectrum shown here (Figure 26) is τ_d - {$(\pi)_x$ - τ - $(\pi/2)_x$ - τ_1 - $(\pi/2)_y$ - τ_2 - ACQ}. The π_x pulse rotates the magnetization, initially along z, to -z. The magnetization following the $(\pi/2)_x$ pulse depends on the value of τ. With $\tau = 0$, the pulse sequence is equivalent to a single $3\pi/2$ pulse and an inverted spectrum is observed, while for $\tau \geq 5T_{1Z}$, the magnetization recovers fully between the $(\pi)_x$ and $(\pi/2)_x$ pulses and a standard spectrum is observed. The recycle delay, τ_d, must be set to a value greater than 5 T_1 to allow full recovery of the magnetization between transients. The value of τ for which no signal is observed (τ_{null}) may be used to estimate T_{1Z} according to $T_{1Z} \approx \tau_{null}/(\ln 2)$.[41,287] Proper analysis

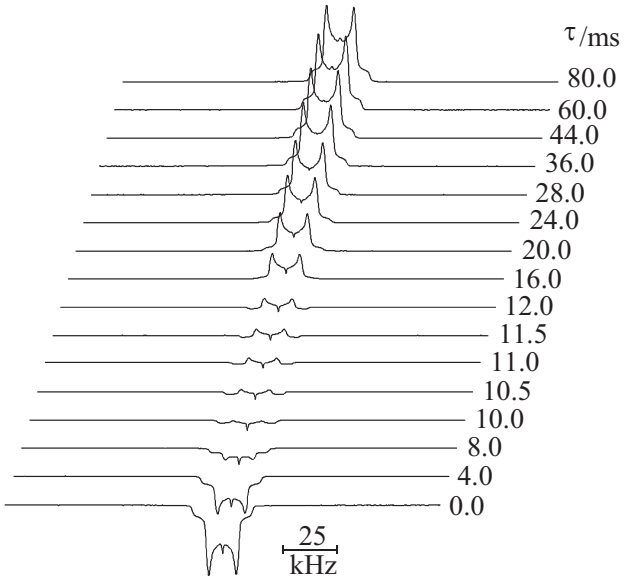

Figure 26: Deuterium NMR spectra of a stationary sample of trimethylamine-d_9·HCl, acquired at 9.4 T with various values of τ. A standard inversion-recovery pulse sequence was modified to include the quadrupolar echo (see text), with $\tau_1 = 17$ μs, $\tau_2 = 9$ μs, $\pi/2 = 2.3$ μs. Sixteen transients were acquired and a recycle delay of 4 s was used for each spectrum.

of inversion recovery data necessitates full excitation of the sample so that the magnetization is completely inverted by the π pulse. Composite inversion pulses[287] have been suggested to ensure complete excitation of broad spectra. The signal intensity $S(t)$ is fit to either a two-parameter or three-parameter model, with the latter being preferable.[41,287,307] As for other properties of solids, T_{1Z} is usually not isotropic.[292,306] Hence, the inversion recovery should be sampled at various points of the spectrum, particularly in the region of the null. Figure 26 illustrates an inversion recovery experiment carried out on trimethylamine$-d_9$·HCl, $N(CD_3)_3$·HCl. Note that in the region with τ between 10.5 and 12.0 ms, the horns of the spectra yield a positive signal while the shoulders are negative. From these spectra, the isotropic value of T_{1Z} for this compound is estimated to be 19 ms.

The availability of instruments capable of acquiring and processing the broad spectra observed in ^{2}H NMR, combined with computer simulation programs,[289b,308] have contributed to the routine investigation of molecular dynamics by ^{2}H NMR. Such experiments, when carried out at various temperatures, yield information such as barriers to internal rotation, reorientation rates, *etc.*[309] Molecular dynamics are described by the Arrhenius equation, $\ln(\tau/\tau_0) = (E_a/R)(1/T)$, where τ is the correlation time, E_a is the activation energy, and R is the gas constant.[88] If the motion is occurring at a frequency that is comparable to or greater than C_Q, the averaged quadrupolar coupling constant, and η, will be reflected in the observed line shape. This is clearly seen in the spectrum of pmma (Figure 24). The rapid rotation of the CD_3 groups leads to averaging of C_Q, (dotted line) while that for the essentially rigid CD_2 group (dashed line) is unaffected.

The observed line shapes depend on the type of motion.[284d] For example, the line shape observed for CD_3 groups in the intermediate exchange regime depends on whether the group is undergoing discrete three-site jump motion or free diffusion.[310] Caution should be used in drawing conclusions from a single spectrum, since different motions may yield similar spectra. This discrepancy may be resolved by a careful measurement of the relaxation using the inversion recovery experiment described above.[306,311] In addition, one must consider the situation where several types of motion may be occurring simultaneously.[292,312] Although qualitative information about molecular dynamics is available from a single ^{2}H NMR spectrum, a quantitative investigation entails the acquisition of several spectra as a function of temperature.

In this section, the focus has been on the investigation of molecular dynamics *via* ^{2}H NMR. Readers should be aware that information on molecular dynamics is also available from other one- and multi-dimensional NMR techniques.[88,313] For example, 2D exchange NMR can provide information on slow dynamic processes.[314] Information on dynamic behaviour may also be obtained through the measurement of proton line widths and relaxation rates as a function of temperature.[22,88,315]

6 Synopsis

It is hoped that the reader will find this practical guide to routine one-dimensional solid-state NMR experiments useful. One of the crucial differences between solid-state and solution NMR is that in solids, anisotropic interactions are not averaged by rapid molecular tumbling as they are in solution. This fundamental fact complicates SSNMR spectra and at the same time allows for the extraction of more complete information about the NMR interaction tensors and their relationship with local molecular and electronic structure, as well as molecular dynamics. Using one-dimensional experiments such as those described

herein can afford a wealth of useful information on a wide variety of chemical systems.

7 Acknowledgements

We thank the Natural Sciences and Engineering Research Council of Canada (NSERC) for research grants. NMR spectra (4.7 T and 9.4 T) were acquired at the Atlantic Region Magnetic Resonance Centre (ARMRC), which is supported by NSERC. The 17.63 T spectrum was acquired in the Environmental Molecular Sciences Laboratory (a national scientific user facility sponsored by the U.S. DOE Office of Biological and Environmental Research) located at Pacific Northwest National Laboratory, operated by Battelle for the DOE. We sincerely thank Brian Millier for his invaluable efforts in maintaining the spectrometers at ARMRC. We thank Tom Nakashima, Glen Bigam, and Ed Feschuk at the University of Alberta. Anil Mehta, Glenn Penner, and Michelle Forgeron are acknowledged for their valuable comments on the manuscript. Previous group members who worked on solid-state NMR projects are gratefully acknowledged: Tom Stringfellow, Jerry C. C. Chan, Glenn Penner, Jim Britten, Mike McKinnon, Scott Kroeker, Robert W. Schurko, Gang Wu, Bill Power, Mark MacIntosh, Ron Curtis, Marco Gruwel, Sandra Mooibroek, Brian Pettitt, and all honours project students. We also value the technical assistance we have received over the years from the spectrometer manufacturers, in particular Jim Frye (Chemagnetics), Cindy Ridenour (Chemagnetics), and Stan Woodman (Bruker). R.E.W. is a Canada Research Chair in physical chemistry. D.L.B. and M.G. thank NSERC, Dalhousie University, the Izaak Walton Killam Trust, and the Walter C. Sumner Foundation for post-graduate scholarships.

8 References

1. From The Institute for Scientific Information's "Web of Science", http://wos.isiglobalnet.com/.
2. (a) *NMR Basic Princ. Prog.,* **29** (1993). (b) *NMR Basic Princ. Prog.,* **30** (1994). (c) *NMR Basic Princ. Prog.,* **31** (1994). (d) *NMR Basic Princ. Prog.,* **32** (1994). (e) *NMR Basic Princ. Prog.,* **33** (1994).
3. N. J. Clayden, *Annu. Rep. NMR Spectrosc.* **24**, 1 (1992).
4. C. Ye, S. Ding and C. A. McDowell, *Annu. Rep. NMR Spectrosc.*, **42**, 58 (2000).
5. H. Eckert, *Prog. Nucl. Magn. Reson. Spectrosc.*, **24**, 159 (1992).
6. S. Hayashi, *Annu. Rep. NMR Spectrosc.,* **28**, 29 (1994).
7. H. Kawazoe, *Annu. Rep. NMR Spectrosc.*, **28**, 1 (1994).
8. H. Pfeifer and H. Ernst, *Annu. Rep. NMR Spectrosc.*, **28**, 91 (1994).
9. F. D. Blum, *Annu. Rep. NMR Spectrosc.*, **28**, 277 (1994).
10. N. Asakawa, T. Kameda, S. Kuroki, H. Kurosu, S. Ando, I. Ando and A. Shoji, *Annu. Rep. NMR Spectrosc.*, **35**, 55 (1998).
11. J. H. Davis and M. Auger, *Prog. Nucl. Magn. Reson. Spectrosc.*, **35**, 1 (1999).
12. K. Saito, K. Kanehashi and I. Komaki, *Annu. Rep. NMR Spectrosc.*, **44**, 23 (2001).
13. K. Asayama, Y. Kitaoka, G-q. Zheng, K. Ishida and Y. Tokunaga, *Annu. Rep. NMR Spectrosc.*, **44**, 75 (2001).
14. For the most recent review, see: C. Dybowski and S. Bai, *Anal. Chem.*, **72**, 1R (2000).
15. C. A. Fyfe, "*Solid State NMR for Chemists"*, C. F. C. Press, Guelph, ON, 1983.
16. J. A. Ripmeester and C. I. Ratcliffe, In "*Comprehensive Supramolecular Chemistry*", Vol. 8, J. L. Atwood, J. E. D. Davies, D. D. MacNicol and F. Vogtle, Eds., Pergamon Press, Amsterdam, 1996, chapter 8.
17. J. J. Fitzgerald and S. M. DePaul, In "*Solid-State NMR Spectroscopy of Inorganic Materials*", ACS Symposium Series 717, J. J. Fitzgerald, Ed., Oxford University Press, 1999, chapter 1.
18. S. Dusold and A. Sebald, *Annu. Rep. NMR Spectrosc.*, **41**, 185 (2000).
19. K. Eichele and R. E. Wasylishen, *WSOLIDS NMR Simulation Package*, 2001. See http://ramsey.chem.ualberta.ca/programs.html and http://casgm3.anorg.chemie.uni-tuebingen.de/klaus/soft/index.html
20. E. Fukushima and S. B. W. Roeder, "*Experimental Pulse NMR: A Nuts and Bolts Approach*", Addison-Wesley Publishing Company, Inc., Massachusetts, 1981.
21. D. Shaw, "*Fourier Transform N.M.R. Spectroscopy*", 2nd ed., Elsevier Science Publishing Company Inc., New York, 1984.
22. T. C. Farrar and E. D. Becker, "*Pulse and Fourier*

Transform NMR: Introduction to Theory and Methods", Academic Press Inc., New York, 1971.
23. M. L. Martin, J. J. Delpuech and G. J. Martin, "*Practical NMR Spectroscopy*", Heydon & Son Ltd., Philadelphia, PA, 1980.
24. H. D. W. Hill, In "*Encyclopedia of Nuclear Magnetic Resonance"*, D. M. Grant and R. K. Harris, Eds., John Wiley & Sons, New York, 1996, p. 4505.
25. R. E. Wasylishen, In "*Encyclopedia of Nuclear Magnetic Resonance"*, D. M. Grant and R. K. Harris, Eds., John Wiley & Sons, New York, 1996, p.1685.
26. D. L. VanderHart, W. L. Earl and A. N. Garroway, *J. Magn. Reson.*, **44**, 361 (1981).
27. (a) *The ARRL Handbook for Radio Amateurs*, The American Radio Relay League,Newington, CT, 1999, Chapter 13, p. 13.2. (b) H. Förster, "*AVANCE DMX/DSX Spectrometers - Solids Experiments User Manual - Version 001*", Bruker Analytik GmbH, 1996.
28. E. R. Andrew, *Prog. Nucl. Magn. Reson. Spectrosc.*, **8**, 1 (1972).
29. U. Haeberlen, In *"Advances in Magnetic Resonance"*, Supplement 1, J. S. Waugh, Ed., Academic Press, New York, 1976.
30. C. S. Yannoni, *Acc. Chem. Res.*, **15**, 201 (1982).
31. M. Mehring, "*Principles of High Resolution NMR in Solids*", 2nd ed., Springer-Verlag, Berlin, 1983.
32. E. O. Stejskal and J. D. Memory, "*High Resolution NMR in the Solid State: Fundamentals of CP/MAS*", Oxford University Press, New York, 1994.
33. L. Chopin, R. Rosanske and T. Gullion, *J. Magn. Reson.*, **122A**, 237 (1996).
34. F. D. Doty, G. Entzminger and Y. A. Yang, *Concepts Magn. Reson.*, **10**, 133 and 239 (1998).
35. F. D. Doty, In "*Encyclopedia of Nuclear Magnetic Resonance*", D. M. Grant and R. K. Harris, Eds., John Wiley & Sons, New York, 1996, p.3753 and 4475.
36. Y. J. Jiang, *J. Magn. Reson.*, **142**, 386 (2000) and references therein.
37. (a) Release Notes: 2.5 mm MAS System, Bruker Analytik, 1997. (b) B. Langer, I. Schnell, H. W. Spiess and A.-R. Grimmer, *J. Magn. Reson.*, **138**, 182 (1999).
38. A. E. Derome, "*Modern NMR Techniques for Chemistry Research*", Pergamon Press, New York, 1987.
39. S. R. Hartmann and E. L. Hahn, *Phys. Rev.*, **128**, 2042 (1962).
40. Naval Air Warfare Center Weapons Division Web site: http://ewhdbks.mugu.navy.mil/dutycy.htm, accessed May 2001.
41. R. K. Harris, "*Nuclear Magnetic Resonance Spectroscopy - A Physicochemical View*", Longman Scientific & Technical, Essex, 1994.
42. J. K. M. Sanders and B. K. Hunter, "*Modern NMR Spectroscopy: A Guide for Chemists*", 2nd edition, Oxford University Press, New York, 1993.
43. D. D. Traficante, In "*NMR Spectroscopy Techniques"*, 2nd ed., M. D. Bruch, Ed., Marcel Dekker, Inc., New York, 1996.
44. See for example: T. D. W. Claridge, "*High-Resolution NMR Techniques in Organic Chemistry*", Pergamon, Amsterdam, 1999, chapter 3.
45. A. D. Bain and I. W. Burton, *Concepts Magn. Reson.,* **3**, 191 (1996).
46. A. G. Marshall and F. R. Verdun, "*Fourier Transforms in NMR, Optical, and Mass Spectrometry*", Elsevier Science Publishing Company Inc., New York, 1990.
47. J. C. Hoch and A. S. Stern, "*NMR Data Processing*", Wiley-Liss Inc., New York, 1996.
48. D. Canet, "*Nuclear Magnetic Resonance: Concepts and Methods*", John Wiley & Sons, New York, 1996.
49. P. A. Keifer, *Concepts Magn. Reson.*, **11**, 165 (1999).
50. J. Mason, *Solid State Nucl. Magn. Reson.*, **2**, 285 (1993).
51. D. L. VanderHart and H. S. Gutowsky, *J. Chem. Phys.*, **49**, 261 (1968).
52. D. L. VanderHart, H. S. Gutowsky and T. C. Farrar, *J. Chem. Phys.*, **50**, 1058 (1969).
53. M. Linder, A. Höhener and R. R. Ernst, *J. Chem. Phys.*, **73**, 4959 (1980).
54. K. W. Zilm and D. M. Grant, *J. Am. Chem. Soc.*, **103**, 2913 (1981).
55. R. E. Wasylishen, R. D. Curtis, K. Eichele, M. D. Lumsden, G. H. Penner, W. P. Power and G. Wu, In "*Nuclear Magnetic Shieldings and Molecular Structure*", NATO Series C: Mathematical and Physical Sciences - Vol. 386, J. A. Tossell, Ed, Kluwer Academic Publishers, Dordrecht, 1993, p.297.
56. E. L. Hahn, *Phys. Rev.*, **80**, 580 (1950).
57. (a) H. Y. Carr and E. M. Purcell, *Phys. Rev.*, **94**, 630 (1954); (b) S. Meiboom and D. Gill, *Rev. Sci. Instr.*, **29**, 688 (1958).
58. M. E. Stoll, A. J. Vega, and R. W. Vaughan, *J. Chem. Phys.*, **65**, 4093 (1976).

59. R. D. Curtis, *Ph.D. Thesis*, Dalhousie University, 1990.
60. M. Rance and R. A. Byrd, *J. Magn. Reson.*, **52**, 221 (1983).
61. D. L. Bryce and R. E. Wasylishen, *J. Phys. Chem. A*, **104**, 7700 (2000).
62. C. D. Baer, *J. Chem. Educ.,* **67**, 410 (1990).
63. J. Hulliger, *Angew. Chem. Int. Ed. Engl.,* **33**, 143 (1994).
64. P. D. Boyle, website: http://laue.chem.ncsu.edu/web/GrowXtal.html, 1999, and references therein. Accessed May 2001.
65. T. Vosegaard, P. Daugaard, E. Hald and H. J. Jakobsen, *J. Magn. Reson.,* **142**, 379 (2000).
66. T. Vosegaard, E. Hald, V. Langer, H. J. Skov, P. Daugaard, H. Bildsøe and H. J. Jakobsen, *J. Magn. Reson.*, **135**, 126 (1998).
67. C. M. Carter, D. W. Alderman and D. M. Grant. *J. Magn. Reson.*, **65**, 183 (1985).
68. C. M. Carter, D. W. Alderman and D. M. Grant, *J. Magn. Reson.*, **73**, 114 (1987).
69. M. H. Sherwood, D. W. Alderman and D. M. Grant, *J. Magn. Reson.*, **84**, 466 (1989).
70. T. Vosegaard, E. Hald, P. Daugaard and H. J. Jakobsen, *Rev. Sci. Instrum.*, **70**, 1771 (1999).
71. M. A. Kennedy and P. D. Ellis, *Concepts in Magn. Reson.*, **1**, 35 and 109 (1989).
72. S. Kroeker, K. Eichele, R. E. Wasylishen and J. F. Britten, *J. Phys. Chem. B.*, **101**, 3727 (1997).
73. C. A. Fyfe and R. E. Wasylishen, In "*Solid State Chemistry Techniques*", A. K. Cheetham and P. Day, Eds., Clarendon Press, 1987, chapter 6.
74. A. Pines, M. G. Gibby, and J. S. Waugh, *J. Chem. Phys.*, **59**, 569 (1973).
75. A. Sebald, *NMR Basic Princ. Prog.,* **31**, 91 (1994).
76. D. P. Burum, In "*Encyclopedia of Nuclear Magnetic Resonance*", D. M. Grant and R. K. Harris, Eds., John Wiley & Sons, New York, 1996, p. 1535.
77. R. R. Ernst, G. Bodenhausen and A. Wokaun, "*Principles of Nuclear Magnetic Resonance in One and Two Dimensions*", Volume 14 In "*The International Series of Monographs on Chemistry*", R. Breslow, J. B. Goodenough, J. Halpern, and J. S. Rowlinson, Eds., Clarendon Press, Oxford, 1987, Section 4.5.
78. H. Geen, J. J. Titman and H. W. Spiess, *Chem. Phys. Lett.*, **213**, 145 (1993).
79. S. Hediger, P. Signer, M. Tomaselli, R. R. Ernst and B. H. Meier, *J. Magn. Reson.*, **125**, 291 (1997).
80. S. Hediger, B. H. Meier and R. R. Ernst, *J. Chem. Phys.*, **102**, 4000 (1995).
81. S. Hediger, B. H. Meier and R. R. Ernst, *Chem. Phys. Lett.,* **213**, 627 (1993).
82. E. R. Andrew and R. A. Newing, *Proc. Phys. Soc.*, **72**, 959 (1958).
83. E. R. Andrew, In "*Encyclopedia of Nuclear Magnetic Resonance*", D. M. Grant and R. K. Harris, Eds., John Wiley & Sons, New York, 1996, p.2891.
84. E. R. Andrew, A. Bradbury and R. G. Eades, *Nature (London)*, **182**, 1659 (1958).
85. E. R. Andrew, A. Bradbury and R. G. Eades, *Nature (London)*, **183**, 1802 (1959).
86. I. J. Lowe, *Phys. Rev. Lett.*, **2**, 285 (1959).
87. E. R. Andrew, *Phil. Trans. R. Soc. Lond.,* **A299**, 505 (1981).
88. K. Schmidt-Rohr and H. W. Spiess, "*Multidimensional Solid-State NMR and Polymers*", Academic Press, London, 1994.
89. A. E. Bennett, C. M. Rienstra, M. Auger, K. V. Lakshmi and R. G. Griffin, *J. Chem. Phys.*, **103**, 6951 (1995).
90. D. L. VanderHart and G. C. Campbell, *J. Magn. Reson.*, **134**, 88 (1998).
91. Z. Gan and R. R. Ernst, *Solid State Nucl. Magn. Reson.*, **8**, 153 (1997).
92. M. Ernst, S. Bush, A. C. Kolbert and A. Pines, *J. Chem. Phys.*, **105**, 3387 (1996).
93. E. O. Stejskal, J. Schaefer and J. S. Waugh, *J. Magn. Reson.*, **28**, 105 (1977).
94. K. Eichele, S. Kroeker, G. Wu and R. E. Wasylishen, *Solid State Nucl. Magn. Reson.*, **4**, 295 (1995).
95. L. H. Merwin and A. Sebald, *J. Magn. Reson.*, **97**, 628 (1992).
96. E. T. Lippmaa, M. A. Alla, T. J. Pehk and G. Engelhardt, *J. Am. Chem. Soc.*, **100**, 1929 (1978).
97. M. J. Collins, J. A. Ripmeester and J. F. Sawyer, *J. Am. Chem. Soc.*, **109**, 4113 (1987).
98. M. J. Collins, C. I. Ratcliffe and J. A. Ripmeester, *J. Magn. Reson.*, **68**, 172 (1986).
99. R. K. Harris and A. Sebald, *Magn. Reson. Chem.*, **25**, 1058 (1987).
100. F. Ambrosius, E. Klaus, T. Schaller and A. Sebald, *Z. Naturforsch*, **50a**, 423 (1995).
101. T. T. P. Cheung, L. E. Worthington, P. D. Murphy and B. C. Gerstein, *J. Magn. Reson.*, **41**, 158 (1980).
102. (a) P. G. Mennitt, M. P. Shatlock, V. J. Bartuska and G. E. Maciel, *J. Phys. Chem.,* **85**, 2087 (1981). (b) N. G. Charles, E. A. H. Griffith,

P. F. Rodesiler and E. L. Amma, *Inorg. Chem.*, **22**, 2717 (1983).
103. K. Eichele and R. E. Wasylishen, *J. Phys. Chem.,* **98**, 3108 (1994).
104. S. Hayashi and K. Hayamizu, *Magn. Reson. Chem.*, **30**, 658 (1992).
105. (a) S. Hayashi and K. Hayamizu, *Bull. Chem. Soc. Jpn.*, **62**, 2429 (1989). (b) S. Hayashi and K. Hayamizu, *Bull. Chem. Soc. Jpn.*, **64**, 685 (1991).
106. (a) A. Pines and T. W. Shattuck, *J. Chem. Phys.*, **61**, 1255 (1974). (b) W. L. Earl and D. L. VanderHart, *J. Magn. Reson.*, **48**, 35 (1982).
107. M. J. Potrzebowski, P. Tekely and Y. Dusausoy, *Solid State Nucl. Magn. Reson.*, **11**, 253 (1998).
108. C. P. Slichter, "*Principles of Magnetic Resonance*", Springer Series in Solid-State Sciences 1, 3rd edition, Springer-Verlag, Berlin, 1990, Sections 3.3 and 3.4.
109. J. Tegenfeldt and U. Haeberlen, *J. Magn. Reson.*, **36**, 453 (1979).
110. (a) L. B. Alemany, D. M. Grant, R. J. Pugmire, T. D. Alger and K. W. Zilm, *J. Am. Chem. Soc.*, **105**, 2133 (1983). (b) L. B. Alemany, D. M. Grant, R. J. Pugmire, T. D. Alger and K. W. Zilm, *J. Am. Chem. Soc.*, **105**, 2142 (1983). (c) L. B. Alemany, D. M. Grant, T. D. Alger and R. J. Pugmire, *J. Am. Chem. Soc.*, **105**, 6697 (1983).
111. J.-D. Mao, W.-G. Hu, K. Schmidt-Rohr, G. Davies, E. A. Ghabbour and B. King, *Soil Sci. Soc. Am. J.*, **64**, 873 (2000) and references therein.
112. B. Wrackmeyer and R. Contreras, *Annu. Rep. NMR Spectrosc.*, **24**, 267 (1992).
113. G. A. Bowmaker, R. K. Harris and S.-W. Oh, *Coord. Chem. Rev.*, **167**, 49 (1997).
114. C. H. Klein Douwel, W. E. J. R. Maas, W. S. Veeman, G. H. Werumeus Buning and J. M. J. Vankan, *Macromolecules*, **23**, 406 (1990).
115. A. Sebald, L. H. Merwin, T. Schaller and W. Knöller, *J. Magn. Reson.*, **96**, 159 (1992).
116. J. Schaefer, R. A. McKay and E. O. Stejskal, *J. Magn. Reson.*, **34**, 443 (1979).
117. M. Sardashti and G. E. Maciel, *J. Magn. Reson.*, **72**, 467 (1987).
118. O. B. Peersen, X. Wu, I. Kustanovich and S. O. Smith, *J. Magn. Reson.*, **A104**, 334 (1993).
119. O. B. Peersen, X. Wu and S. O. Smith, *J. Magn. Reson.*, **A106**, 127 (1994).
120. G. Metz, X. Wu and S. O. Smith, *J. Magn. Reson.*, **A110**, 219 (1994)
121. (a) T. M. Barbara and E. H. Williams, *J. Magn. Reson.,* **99**, 439 (1992); (b) X. Wu and K. W. Zilm, *J. Magn. Reson.*, **A104**, 154 (1993).
122. B. Q. Sun, P. R. Costa and R. G. Griffin, *J. Magn. Reson.*, **A112**, 191 (1995).
123. A. C. Kolbert and S. L. Gann, *Chem. Phys. Lett.*, **224**, 86 (1994).
124. J. Herzfeld and A. E. Berger, *J. Chem. Phys.*, **73**, 6021 (1980).
125. M. M. Maricq and J. S. Waugh, *J. Chem. Phys.*, **70**, 3300 (1979).
126. T. M. de Swiet, M. Tomaselli and A. Pines, *Chem. Phys. Lett.,* **285**, 59 (1998).
127. W. T. Dixon, J. Schaefer, M. D. Sefcik, E. O. Stejskal and R. A. McKay, *J. Magn. Reson.*, **45**, 173 (1981).
128. W. T. Dixon, J. Schaefer, M. D. Sefcik, E. O. Stejskal and R. A. McKay, *J. Magn. Reson.*, **49**, 341 (1982).
129. W. T. Dixon, *J. Chem. Phys.*, **77**, 1800 (1982).
130. N. Chr. Nielsen, H. Bildsøe and H. J. Jakobsen, *J. Magn. Reson.*, **80**, 149 (1988).
131. H. Geen and G. Bodenhausen, *J. Chem. Phys.*, **97**, 2928 (1992).
132. H. Geen, M. H. Levitt and G. Bodenhausen, *Chem. Phys. Lett.*, **200**, 350 (1992).
133. Z. Song, O. N. Antzutkin, X. Feng and M. H. Levitt, *Solid State Nucl. Magn. Reson.*, **2**, 143 (1993).
134. J. Hong and G. S. Harbison, *J. Magn. Reson.*, **A105**, 128 (1993).
135. H. Geen and G. Bodenhausen, *J. Am. Chem. Soc.*, **115**, 1579 (1993).
136. T. J. Bonagamba and H. Panepucci, *J. Magn. Reson.*, **A103**, 103 (1993).
137. E. T. Olejniczak, S. Vega and R. G. Griffin, *J. Chem. Phys.*, **81**, 4804 (1984).
138. D. P. Raleigh, E. T. Olejniczak, S. Vega and R. G. Griffin, *J. Magn. Reson.*, **72**, 238 (1987).
139. D. P. Raleigh, A. C. Kolbert and R. G. Griffin, *J. Magn. Reson.*, **89**, 1 (1990).
140. O. N. Antzutkin and M. H. Levitt, *J. Magn. Reson.*, **A118**, 295 (1996).
141. D. P. Raleigh, E. T. Olejniczak and R. G. Griffin, *J. Chem. Phys.*, **89**, 1333 (1988).
142. J. Leppert, B. Heise and R. Ramachandran, *J. Magn. Reson.*, **139**, 382 (1999).
143. Y. J. Jiang, R. J. Pugmire and D. M. Grant, *J. Magn. Reson.*, **71**, 485 (1987).
144. T. K. Pratum, *J. Magn. Reson.*, **88**, 384 (1990).
145. E. Brunner, D. Freude, B. C. Gerstein and H. Pfeifer, *J. Magn. Reson.*, **90**, 90 (1990).

146. J. R. Sachleben, S. Caldarelli and L. Emsley, *J. Chem. Phys.*, **104**, 2518 (1996).
147. P. Tekely, P. Palmas and D. Canet, *J. Magn. Reson.*, **107A**, 129 (1994).
148. (a) W. P. Rothwell and J. S. Waugh, *J. Chem. Phys.*, **74**, 2721 (1981). (b) D. E. Warschawski, J. D. Gross and R. G. Griffin, *J. Chim. Phys.*, **95**, 460 (1998) and references therein.
149. G. Metz, M. Ziliox and S. O. Smith, *Solid State Nucl. Magn. Reson.*, **7**, 155 (1996).
150. A. Lesage, S. Steuernagel and L. Emsley, *J. Am. Chem. Soc.*, **120**, 7095 (1998).
151. A. Lesage, D. Sakellariou, S. Steuernagel and L. Emsley, *J. Am. Chem. Soc.*, **120**, 13194 (1998).
152. S. J. Opella and M. H. Frey, *J. Am. Chem. Soc.*, **101**, 5854 (1979).
153. J. S. Hartman and J. A. Ripmeester, *Chem. Phys. Lett.*, **168**, 219 (1990).
154. R. Sangill, N. Rastrup-Andersen, H. Bildsøe, H. J. Jakobsen and N. C. Nielsen, *J. Magn. Reson.*, **107A**, 67 (1994).
155. S. T. Burns, *Ph.D. Thesis*, Yale University, 1998.
156. S. T. Burns, X. L. Wu and K. W. Zilm, *J. Magn. Reson.*, **143**, 352 (2000).
157. M. Baldus, A. T. Petkova, J. Herzfeld and R. G. Griffin, *Mol. Phys.*, **95**, 1197 (1998).
158. Of course, one should ensure that the applied magnetic field is homogeneous. It should be noted that strategies for shimming MAS probes are different from shimming standard liquid probes. See A. Sodickson and D. G. Cory, *J. Magn. Reson.*, **128**, 87 (1997).
159. D. E. Axelson, "*Solid State Nuclear Magnetic Resonance of Fossil Fuels*", Multiscience Publications Ltd., Canada, 1985, Chapter 4.
160. J. S. Frye and G. E. Maciel, *J. Magn. Reson.*, **48**. 125 (1982).
161. A. Kubo and C. A. McDowell, *J. Magn. Reson.*, **92**, 409 (1991).
162. G. Wu and R. E. Wasylishen, *J. Chem. Phys.*, **100**, 4828 (1994).
163. R. C. Crosby and J. F. Haw, *J. Magn. Reson.*, **82**, 367 (1989).
164. C. S. Nagaraja and K. V. Ramanathan, *J. Magn. Reson.*, **146**, 165 (2000).
165. C. L. Khetrapal, B. S. A. Kumar, K. V. Ramanathan and N. Suryaprakash, *J. Magn. Reson.*, **73**, 516 (1987).
166. E. B. Brouwer, R. Challoner and R. K. Harris, *Solid State Nucl. Magn. Reson.*, **18**, 37 (2000).
167. R. K. Harris, In "*Encyclopedia of Nuclear Magnetic Resonance*", D. M. Grant and R. K. Harris, Eds., John Wiley & Sons, Chichester, 1996, p 3301.
168. P. L. Goggin, R. J. Goodfellow and F. J. S. Reed, *J. Chem. Soc., Dalton*, 576 (1974).
169. S. Hayashi and K. Hayamizu, *Bull. Chem. Soc. Jpn.*, **64**, 688 (1991).
170. R. E. Wasylishen, unpublished results.
171. S. Ando, R. K. Harris and S. A. Reinsberg, *J. Magn. Reson.*, **141**, 91 (1999).
172. G. Neue, C. Dybowski, M. L. Smith, M. A. Hepp and D. L. Perry, *Solid State Nucl. Magn. Reson.*, **6**, 241 (1996).
173. C. Brevard and P. Granger, "*Handbook of High Resolution Multinuclear NMR*", John Wiley & Sons, New York, 1981.
174. A. Carrington and A. D. McLachlan, "*Introduction to Magnetic Resonance*", Harper & Row, New York, 1967, p.42.
175. J. P. Yesinowski and H. Eckert, *J. Am. Chem. Soc.*, **109**, 6274 (1987).
176. P. J. Giammatteo, W. W. Hellmuth, F. G. Ticehurst, and P. W. Cope, *J. Magn. Reson.* **71**, 147 (1987) and references therein.
177. I. D. Gay, *J. Magn. Reson.*, **58**, 413 (1984).
178. L. H. Merwin, A. Sebald, J. E. Espidel and R. K. Harris, *J. Magn. Reson.*, **84**, 367 (1989).
179. L. C. M. v. Gorkom, J. M. Hook, M. B. Logan, J. V. Hanna and R. E. Wasylishen, *Magn. Reson. Chem.,* **33**, 791 (1995).
180. T. Mildner, H. Ernst and D. Freude, *Solid State Nucl. Magn. Reson.*, **5**, 269 (1995).
181. A. Bielecki and D. P. Burum, *J. Magn. Reson.*, **116A**, 215 (1995).
182. P. A. Beckmann and C. Dybowski, *J. Magn. Reson.*, **146**, 379 (2000).
183. B. Wehrle, F. Aguilar-Parrilla and H.-H. Limbach, *J. Magn. Reson.,* **87**, 584 (1990).
184. F. Aguilar-Parrilla, B. Wehrle, H. Bräunling and H.-H. Limbach, *J. Magn. Reson.,* **87**, 592 (1990).
185. C. P. Grey, A. K. Cheetham and C. M. Dobson, *J. Magn. Reson.*, **101A**, 299 (1993).
186. G.-J. M. P. van Moorsel, E. R. H. van Eck and C. P. Grey, *J. Magn. Reson.*, **113A**, 159(1995).
187. B. C. Gerstein, In *"Encyclopedia of Nuclear Magnetic Resonance"*, D. M. Grant and R. K. Harris, Eds., John Wiley & Sons, New York, 1996, p. 1501.
188. Z. Zhou, B. G. Sayer, R. E. Stark and R. M. Epand, *Chem. Phys. Lipids*, **90**, 45 (1997).
189. I. Schnell, S. P. Brown, H. Y. Low, H. Ishida and H. W. Spiess, *J. Am. Chem. Soc.*, **120**, 11784

(1998).
190. S. P. Brown, I. Schell, J. D. Brand, K. Müllen and H. W. Spiess, *J. Am. Chem. Soc.*, **121**, 6712 (1999).
191. J. Virlet, In *"Encyclopedia of Nuclear Magnetic Resonance"*, D. M. Grant and R. K. Harris, Eds., John Wiley & Sons, New York, 1996, p. 2694.
192. U. Haeberlen, "*High Resolution NMR in Solids*", Academic Press, New York, 1976, Chapter 6.
193. R. K. Harris, P. Jackson, L. H. Merwin, B. J. Say and G. Hägele, *J. Chem. Soc., Faraday Trans. 1*, **84**, 3649 (1988).
194. (a) C. E. Bronnimann, B. L. Hawkins, M. Zhang and G. E. Maciel, *Anal. Chem.*, **60**, 1743 (1988); (b) P. Jackson and R. K. Harris, *Magn. Reson. Chem.*, **26**, 1003, (1988); (c) R. K. Harris and P. Jackson, In *"Multinuclear Resonance in Liquids and Solids - Chemical Applications"*, P. Granger and R. K. Harris, Eds., Kluwer Academic, Dordrecht, 1988, p. 355.
195. (a) D. B. Zax, A. Bielecki, K. W. Zilm, A. Pines and D. P. Weitekamp, *J. Chem. Phys.*, **83**, 4877 (1985). (b) A. Llor and J. Virlet, *J. Chem. Phys.*, **84**, 1257 (1987). (c) A. Llor, Z. Olejniczak, J. Sachleben and A. Pines, *Phys. Rev. Lett.*, **67**, 1989 (1991). (d) A. Llor, Z. Olejniczak and A. Pines, *J. Chem. Phys.*, **103**, 3966 and 3982 (1995).
196. (a) R. Tycko, *J. Magn. Reson.*, **75**, 193 (1987). (b) R. Tycko, *Phys. Rev. Lett.*, **60**, 2734 (1988). (c) R. Tycko, *J. Chem. Phys.*, **92**, 5776 (1990). (d) R. Tycko, G. Dabbagh, J. C. Duchamp and K. W. Zilm, *J. Magn. Reson.*, **89**, 205 (1990).
197. J. S. Waugh, L. M. Huber and U. Haeberlen, *Phys. Rev. Lett.*, **20**, 180 (1968).
198. (a) P. Mansfield, *Phil. Trans. R. Soc. Lond., Ser. A.*, **299**, 479 (1981); (b) W.-K. Rhim, D. D. Elleman, and R. W. Vaughan, *J. Chem. Phys.*, **58**, 1772 (1973).
199. D. P. Burum and W. K. Rhim, *J. Chem. Phys.*, **71**, 944 (1979).
200. A. E. McDermott, F. J. Creuzet, A. C. Kolbert and R. G. Griffin, *J. Magn. Reson.*, **98**, 408 (1992).
201. R. Eckman, *J. Chem. Phys.*, **76**, 2767 (1982).
202. C. I. Ratcliffe, J. A. Ripmeester and J. S. Tse, *Chem. Phys. Lett.*, **120**, 427 (1985).
203. G. Wu, C. J. Freure and E. Verdurand, *J. Am. Chem. Soc.*, **120**, 13187 (1998).
204. M. E. Smith and E. R. H. van Eck, *Prog. Nucl. Magn. Reson. Spectrosc.*, **34**, 159 (1999).
205. A. P. M. Kentgens, *Geoderma,* **80**, 271 (1997).
206. M. H. Cohen and F. Reif, In "*Solid State Physics*", Volume 5, F. Seitz and D. Turnbull, Eds., Academic Press, New York, 1957, pp. 321-438.
207. R. V. Pound, *Phys. Rev.*, **79**, 685 (1950).
208. For an extension of Pound's work, see: G. M. Volkoff, H. E. Petch and D. W. L. Smellie, *Can. J. Phys.*, **30**, 270 (1952).
209. A. Abragam, *"The Principles of Nuclear Magnetism"*, Oxford University Press, Oxford, 1961.
210. D. Freude and J. Haase, *NMR Basic Princ. Prog.*, **29**, 1 (1993).
211. F. Taulelle, In "*Multinuclear Magnetic Resonance in Liquids and Solids - Chemical Applications"*, P. Granger and R. K. Harris, Eds., Kluwer Academic Publishers, Dordrecht, 1990, pp 393-407.
212. P. P. Man, In "*Encyclopedia of Nuclear Magnetic Resonance*", D. M. Grant and R. K. Harris, Eds., John Wiley and Sons, New York, 1996, p. 3838.
213. L. van Wüllen, H. Eckert and G. Schwering, *Chem. Mater.*, **12**, 1840 (2000).
214. K. Eichele, R. E. Wasylishen and J. H. Nelson, *J. Phys. Chem. A*, **101**, 5463 (1997).
215. S. Mooibroek, R. E. Wasylishen, R. Dickson, G. Facey and B. A. Pettitt, *J. Magn. Reson.*, **66**, 542 (1986).
216. A. Samoson and E. Lippmaa, *Phys. Rev. B*, **28**, 6567 (1983).
217. P. P. Man, J. Klinowski, A. Trokiner, H. Zanni and P. Papon, *Chem. Phys. Lett.*, **151**, 143 (1988).
218. K. Eichele, J. C. C. Chan, R. E. Wasylishen and J. F. Britten, *J. Phys. Chem. A*, **101**, 5423 (1997).
219. A. J. Woo, D.-Y. Han and S. H. Cho, *Bull. Korean Chem. Soc.*, **21**, 233 (2000).
220. S. Vega, *Phys. Rev. A*, **23**, 3152 (1981).
221. D. E. Woessner, *Z. Phys. Chem.*, **152**, 51 (1987).
222. T. H. Walter, G. L. Turner and E. Oldfield, *J. Magn. Reson.*, **76**, 106 (1988).
223. (a) H. D. Morris and P. D. Ellis, *J. Am. Chem. Soc.*, **111**, 6045 (1989). (b) H. D. Morris, S. Bank and P. D. Ellis, *J. Phys. Chem.*, **94**, 3121 (1990).
224. J. C. Edwards and P. D. Ellis, *Magn. Reson. Chem.*, **28**, S59 (1990).
225. P. J. Barrie, *Chem. Phys. Lett.*, **208**, 486 (1993).
226. S. Ding and C. A. McDowell, *J. Magn. Reson.*, **114A**, 80 (1995).
227. (a) L. Frydman and J. S. Harwood, *J. Am. Chem. Soc.*, **117**, 5367 (1995). (b) A. Medek, J. S. Harwood and L. Frydman, *J. Am. Chem. Soc.*, **117**, 12779 (1995). (c) A. Medek and L.

Frydman, *J. Braz. Chem. Soc.*, **10**, 263 (1999).
228. (a) M. Pruski, D. P. Lang, C. Fernandez and J. P. Amoureux, *Solid State Nucl. Magn. Reson.,* **7**, 327 (1997). (b) C. Fernandez, L. Delevoye, J.-P. Amoureux, D. P. Lang and M. Pruski, *J. Am. Chem. Soc.,* **119**, 6858 (1997).
229. See, for example: (a) S. E. Ashbrook, S. P. Brown and S. Wimperis, *Chem. Phys. Lett.,* **288**, 509 (1998). (b) S. E. Ashbrook and S. Wimperis, *Mol. Phys.,* **98**, 1 (2000).
230. See, for example: (a) K. H. Lim and C. P. Grey, *Chem. Phys. Lett.,* **312**, 45 (1999). (b) K. H. Lim and C. P. Grey, *J. Chem. Phys.,* **112**, 7490 (2000).
231. D. Rovnyak, M. Baldus and R. G. Griffin, *J. Magn. Reson.,* **142**, 145 (2000).
232. M. A. Eastman, *J. Magn. Reson.,* **139**, 98 (1999).
233. J. C. C. Chan, M. Bertmer and H. Eckert, *Chem. Phys. Lett.*, **292**, 154 (1998).
234. S. M. De Paul, M. Ernst, J. S. Shore, J. F. Stebbins and A. Pines, *J. Phys. Chem. B*, **101**, 3240 (1997).
235. K. Narita, J. Umeda and H. Kusumoto, *J. Chem. Phys.,* **44**, 2719 (1966).
236. A. J. Vega, In *"Encyclopedia of Nuclear Magnetic Resonance"*, D. M. Grant and R. K. Harris, Eds., John Wiley & Sons, New York, 1996, p. 3869.
237. P. Granger, *Magn. Reson. Chem.*, **28**, 156 (1989).
238. J. P. Amoureux, C. Fernandez and P. Granger, In "*Multinuclear Magnetic Resonance in Liquids and Solids - Chemical Applications*", NATO ASI Series C - Vol. 322, P. Granger and R. K. Harris, Eds., Kluwer Academic Publishers, Dordrecht, 1990, chapter XXII.
239. J. C. C. Chan, *Concepts Magn. Reson.*, **11**, 363 (1999).
240. A. C. Kunwar, G. L. Turner and E. Oldfield, *J. Magn. Reson.*, **69**, 124 (1986).
241. M. E. Smith, *Annu. Rep. Nucl. Magn. Spectrosc.*, **43**, 121 (2000).
242. M. E. Smith and J. H. Strange, *Meas. Sci. Technol.*, **7**, 449 (1996).
243. J. Haase and E. Oldfield, *J. Magn. Reson.*, **101A**, 30 (1993).
244. (a) P. P. Man, *J. Magn. Reson.*, **100**, 157 (1992). (b) P. P. Man, *J. Magn. Reson.* **114A**, 59 (1995).
245. P. R. Bodart, J.-P. Amoureux, Y. Dumazy and R. Lefort, *Mol. Phys.*, **98**, 1545 (2000).
246. J. T. Cheng and P. D. Ellis, *J. Phys. Chem.*, **93**, 2549 (1989).
247. F. H. Larsen, H. J. Jakobsen, P. D. Ellis and N. Chr. Nielsen, *J. Phys. Chem. A*, **101**, 8597 (1997).
248. F. H. Larsen, H. J. Jakobsen, P. D. Ellis and N. Chr. Nielsen, *Mol. Phys.*, **95**, 1185 (1998)
249. F. H. Larsen, H. J. Jakobsen, P. D. Ellis and N. Chr. Nielsen, *J. Magn. Reson.*, **131**, 144 (1998).
250. F. H. Larsen, A. S. Lipton, H. J. Jakobsen, N. Chr. Nielsen and P. D. Ellis, *J. Am. Chem. Soc.*, **121**, 3783 (1999).
251. F. H. Larsen, J. Skibsted, H. J. Jakobsen and N. Chr. Nielsen, *J. Am. Chem. Soc.*, **122**, 7080 (2000).
252. W. H. Jones, Jr., T. P. Graham and R. G. Barnes, *Phys. Rev.*, **132**, 1898 (1963).
253. J. F. Baugher, P. C. Taylor, T. Oja and P. J. Bray, *J. Chem. Phys.*, **50**, 4914 (1969).
254. W. P. Power, R. E. Wasylishen, S. Mooibroek, B. A. Pettitt and W. Danchura, *J. Phys. Chem.*, **94**, 591 (1990).
255. D. R. Torgeson, R. J. Schoenberger and R. G. Barnes, *J. Magn. Reson.*, **68**, 85 (1986).
256. R. W. Schurko, R. E. Wasylishen and A. D. Phillips, *J. Magn. Reson.*, **133**, 388 (1998).
257. (a) E. Kundla, A Samoson and E. Lippmaa, *Chem. Phys. Lett.*, **83**, 229 (1981); (b) A. Samoson, E. Kundla and E. Lippmaa, *J. Magn. Reson.*, **49**, 350 (1982).
258. H.-J. Behrens and B. Schnabel, *Physica*, **114B**, 185 (1982).
259. A. Samoson, *Chem. Phys. Lett.*, **119**, 29 (1985).
260. D. Freude, J. Haase, J. Klinowski, T. A. Carpenter and G. Ronikier, *Chem. Phys. Lett.,* **119**, 365 (1985).
261. (a) E. Oldfield, S. Schramm, M. D. Meadows, K. A. Smith, R. A. Kinsey and J. Ackerman, *J. Am. Chem. Soc.*, **104**, 919 (1982). (b) S. Schramm and E. Oldfield, *J. Chem. Soc., Chem. Commun.*, 980 (1982). (c) S. Ganapathy, S. Schramm and E. Oldfield, *J. Chem. Phys.*, **77**, 4360 (1982). (d) S. Ganapathy, J. Shore and E. Oldfield, *Chem. Phys. Lett.*, **169**, 301 (1990).
262. (a) F. Lefebvre, J.-P. Amoureux, C. Fernandez and E. G. Derouane, *J. Chem. Phys.*, **86**, 6070 (1987). (b) J. P. Amoureux, C. Fernandez and F. Lefebvre, *Magn. Reson. Chem.*, **28**, 5 (1990).
263. (a) H. J. Jakobsen, J. Skibsted, H. Bildsøe and N. C. Nielsen, *J. Magn. Reson.*, **85**, 173 (1989). (b) J. Skibsted, N. C. Nielsen, H. Bildsøe and H. J. Jakobsen, *J. Magn. Reson.*, **95**, 88 (1991).
264. C. Jäger, *NMR Basic Princ. Prog.*, **31**, 133 (1994).

265. W. P. Power, *Magn. Reson. Chem.*, **33**, 220 (1995).
266. (a) C. Jäger, K. Herzog, B. Thomas, M. Feike and G. Kunath-Fandrei, *Solid State Nucl. Magn. Reson.*, **5**, 51 (1995). (b) K. Herzog, J. Peters, B. Thomas and C. Jäger, *Ber.Bunsen. Ges.*, **100**, 1655 (1996). (c) G. Kunath-Fandrei, D. Ehrt and C. Jäger, *Z. Naturforsch. A*, **50**, 413 (1995).
267. (a) C. Jäger, W. Müller-Warmuth, C. Mundus and L. van Wüllen, *J. Non-Cryst. Sol.*, **149**, 209 (1992). (b) S. W. Ding and C. A. McDowell, *Chem. Phys. Lett.*, **333**, 413 (2001). (c) C. Jäger, *J. Magn. Reson.*, **99**, 353 (1992).
268. (a) A. Samoson, E. Lippmaa and A. Pines, *Mol. Phys.*, **65**, 1013 (1988). (b) Y. Wu, B. Q. Sun, A. Pines, A. Samoson and E. Lippmaa, *J. Magn. Reson.*, **89**, 297 (1990).
269. (a) A. Llor and J. Virlet, *Chem. Phys. Lett.*, **152**, 248 (1988). (b) B. F. Chmelka, K. T. Mueller, A. Pines, J. Stebbins, Y. Wu and J. W. Zwanziger, *Nature (London)*, **339**, 42 (1989). (c) K. T. Mueller, B. Q. Sun, G. C. Chingas, J. W. Zwanziger, T. Terao and A. Pines, *J. Magn. Reson.*, **86**, 470 (1990). (d) K. T. Mueller, G. C. Chingas and A. Pines, *Rev. Sci. Instrum.*, **62**, 1445 (1991). (e) K. T. Mueller, E. W. Wooten and A. Pines, *J. Magn. Reson.,* **92**, 620 (1991).
270. G. Wu, *Biochem. Cell Biol.*, **76**, 429 (1998).
271. B. F. Chmelka and J. W. Zwanziger, *NMR Basic Princ. Prog.,* **33**, 79 (1994).
272. For a description of the sidebands in DAS and DOR experiments, see: B. Q. Sun, J. H. Baltisberger, Y. Wu, A. Samoson and A. Pines, *Solid State Nucl. Magn. Reson.*, **1**, 267 (1992).
273. T. Vosegaard, J. Skibsted and H. J. Jakobsen, *J. Phys. Chem. A*, **103**, 9144 (1999).
274. T. Vosegaard, J. Skibsted, H. Bildsøe and H. J. Jakobsen, *Solid State Nucl. Magn. Reson.*, **14**, 203 (1999).
275. T. Vosegaard, I. P. Byriel and H. J. Jakobsen, *J. Phys. Chem. B*, **101**, 8955 (1997).
276. T. Vosegaard, I. P. Byriel, L. Binet, D. Massiot and H. J. Jakobsen, *J. Am. Chem. Soc.*, **120**, 8184 (1998).
277. T. Vosegaard, I. P. Byriel, D. A. Pawlak, K. Wozniak and H. J. Jakobsen, *J. Am. Chem. Soc.*, **120**, 7900 (1998).
278. T. Vosegaard, U. Andersen and H. J. Jakobsen, *J. Am. Chem. Soc.*, **121**, 1970 (1999).
279. W. P. Power, S. Mooibroek, R. E. Wasylishen, and T. S. Cameron, *J. Phys. Chem.*, **98**, 1552 (1994).
280. A. J. Woo, *Bull. Kor. Chem. Soc.*, **20**, 1205 (1999).
281. W. P. Power, C. W. Kirby and N. J. Taylor, *J. Am. Chem. Soc.*, **120**, 9428 (1998).
282. (a) M. L. H. Gruwel and R. E. Wasylishen, *Z. Naturforsch.*, **46a**, 691 (1991). (b) M. R. MacIntosh, M. L. H. Gruwel, K. N. Robertson and R. E. Wasylishen, *Can. J. Chem.*, **70**, 849 (1992). (c) M. L. H. Gruwel and R. E. Wasylishen, *Z. Naturforsch.*, **47a**, 1073 (1992). (d) M. R. MacIntosh, B. Fraser, M. L. H. Gruwel, R. E. Wasylishen and T. S. Cameron, *J. Phys. Chem.*, **96**, 8572 (1992). (e) P. S. Sidhu, G. H. Penner, K. R. Jeffrey, B. Zhao, Z. L. Wang and I. Goh, *J. Phys. Chem. B*, **101**, 9087 (1997). (f) A. G. Stepanov, A. A. Shubin, M. V. Luzgin, H. Jobic and A. Tuel, *J. Phys. Chem. B*, **102**, 10860 (1998). (g) J. Senker, H. Jacobs, M. Müller, W. Press and G. Neue, *J. Phys. Chem. B*, **103**, 4497 (1999). (h) M. de Langen and K. O. Prins, *Chem. Phys. Lett.*, **299**, 195 (1999). (i) S.-I. Nishikiori, *J. Incl. Phenom.*, **34**, 331 (1999). (j) X. Xie and S. Hayashi, *J. Phys. Chem. B*, **103**, 5956 (1999).
283. (a) A. F. Thomas, *"Deuterium Labeling in Organic Chemistry"*, Appleton-Century-Crofts, New York, 1971. (b) *"Isotopes in the Physical and Biomedical Sciences*", Vol. 1: Labelled Compounds (Part A), E. Buncel and J. R. Jones, Eds., Elsevier, Amsterdam, 1987.
284. (a) J. H. Pines, In *"Isotopes in the Physical and Biomedical Science"*, Vol. 2, E. Buncel and J. R. Jones, Eds., Elsevier, Amsterdam,1991, Chapter 3. (b) G. L. Hoatson, R. L. Vold, *NMR Basic Princ. Prog.*, **32**, 1 (1994). (c) R. Tycko, In *"Understanding Chemical Reactivity"*, Vol. 8, P. G. Mezey, Ed., Kluwer Academic Publishers, Dordrecht, 1994. (d) L. S. Batchelder, In *"Encyclopedia of Nuclear Magnetic Resonance"*, D. M. Grant and R. K. Harris, Eds., John Wiley & Sons, Chichester, 1996, p. 1574. (e) N. Chandrakumar, *NMR Basic Princ. Prog.* **34**, 1 (1996).
285. P. M. Henrichs, J. M. Hewitt and M. Linder, *J. Magn. Reson.*, **60**, 280 (1984).
286. D. Lu, S. Ali and D. J. Siminovitch, *J. Magn. Reson. A*, **122**, 192 (1996).
287. (a) D. J. Siminovitch, D. P. Raleigh, E. T. Olejniczak and R. G. Griffin, *J. Chem. Phys.*, **84**, 2556 (1986). (b) N. J. Heaton, R. R. Vold and R. L. Vold, *J. Magn. Reson.*, **77**, 572 (1988). (c) D. P. Raleigh, E. T. Olejniczak and R. G. Griffin, *J. Magn. Reson.*, **81**, 455 (1989).
288. (a) J. H. Davis, K. R. Jeffrey, M. Bloom, M. I.

Valic and T. P. Higgs, *Chem. Phys. Lett.*, **42**, 390 (1976). (b) M. Bloom, J. H. Davis and M. I. Valic, *Can. J. Phys.*, **58**, 1510 (1980). (c) H. W. Spiess and H. Sillescu, *J. Magn. Reson.*, **42**, 381 (1981).
289. (a) A. D. Ronemus, R. L. Vold and R. R. Vold, *J. Magn. Reson.*, **70**, 416 (1986). (b) M. S. Greenfield, A. D. Ronemus, R. L. Vold, R. R. Vold, P. D. Ellis and T. R. Raidy, *J. Magn. Reson.*, **72**, 89 (1987).
290. R. R. Vold and R. L. Vold, *J. Magn. Reson.*, **70**, 144 (1986).
291. J. A. DiNatale and R. R. Vold, *J. Magn. Reson. A*, **117**, 304 (1995).
292. R. R. Vold and R. L. Vold, *Adv. Magn. Opt. Reson.*, **16**, 85 (1991).
293. A. Müller and U. Haeberlen, *Chem. Phys. Lett.*, **248**, 249 (1996).
294. P. Speier, H. Zimmermann, U. Haeberlen and Z. Luz, *Mol. Phys.*, **95**, 1153 (1998).
295. H. Schmitt, H. Zimmerman, O. Körner, M. Stumber, C. Meinel and U. Haeberlen, *J. Magn. Reson.*, **151**, 65 (2001).
296. C. M. Gall, J. A. DiVerdi and S. J. Opella, *J. Am. Chem. Soc.*, **103**, 5039 (1981).
297. H. W. Spiess, *NMR Basic Princ. Prog.*, **15**, 55 (1978).
298. (a) J. L. Ackerman, R. Eckman and A. Pines, *Chem. Phys.*, **42**, 423 (1979). (b) R. Eckman, M. Alla and A. Pines, *J. Magn. Reson.*, **41**, 440 (1980). (c) J. H. Kristensen, H. Bildsøe, H. J. Jakobsen and N. C. Nielsen, *J. Magn. Reson.,* **100**, 437 (1992). (d) O. Weintraub and S. Vega, *Solid State Nucl. Magn. Reson.*, **4**, 341 (1995).
299. G. H. Penner, Y. C. P. Chang and H. M. Grandin, *Can. J. Chem.*, **77**, 1813 (1999).
300. (a) D. L. VanderHart, W. L. Earl and A. N. Garroway, *J. Magn. Reson.*, **44**, 361 (1981). (b) M. Alla and E. Lippmaa, *Chem. Phys. Lett.*, **87**, 30 (1982). (c) M. A. Hemminga, P. A. De Jager, J. Krüse and R. M. J. N. Lamerichs, *J. Magn. Reson.*, **71**, 446 (1987).
301. (a) M. J. S. Dewar and R. C. Fahey, *J. Am. Chem. Soc.*, **85**, 2704 (1963). (b) K. D. Bartle and D. W. Jones, *J. Mol. Spectrosc.*, **32**, 353 (1969).
302. R. Eckman, L. Müller and A. Pines, *Chem. Phys. Lett.*, **74**, 376 (1980).
303. D. Reichert, Z. Olender, R. Poupko, H. Zimmermann and Z. Luz, *J. Chem. Phys.*, **98**, 7699 (1993).
304. J. P. Jacobsen, H. K. Bildsøe and K. Schaumburg, *J. Magn. Reson.*, **23**, 153 (1976).
305. K. R. Jeffrey, *Bull. Magn. Reson.*, **3**, 69 (1981).
306. D. A. Torchia and A. Szabo, *J. Magn. Reson.*, **49**, *107* (1982).
307. R. E. Wasylishen, In *"NMR Spectroscopy Techniques"*, 2nd Edition, M. D. Bruch, Ed., Practical Spectroscopy Series Volume 21, Marcel Dekker Inc., New York, 1996, chapter 3.
308. (a) L. J. Schwartz, E. Melrovitch, J. A. Ripmeester and J. H. Freed, *J. Phys. Chem.*, **87**, 4453 (1983). (b) P. Meier, E. Ohmes, G. Kothe, A. Blume, J. Weldner and H.-J. Eibl, *J. Phys. Chem.*, **87**, 4904 (1983). (c) R. J. Wittebort, E. T. Olejniczak and R. G. Griffin, *J. Chem. Phys.*, **86**, 5411 (1987).
309. R. G. Griffin, K. Beshah, R. Ebelhäuser, T. H. Huang, E. T. Olejniczak, D. M. Rice, D. J. Siminovitch and R. J. Wittebort, In *"The Time Domain in Surface and Structural Dynamics"*, G. J. Long and F. Grandjean, Eds., NATO ASI Series, Vol. 228, Kluwer Academic Publishers, Dordrecht, 1988, chapter 7.
310. L. S. Batchelder, C. H. Niu and D. A. Torchia, *J. Am. Chem. Soc.*, **105**, 2228 (1983).
311. J. Hirschinger and A. D. English, *J. Magn. Reson.*, **85**, 542 (1989).
312. G. H. Penner and J. M. Polson, *J. Chem. Soc., Dalton Trans.*, 803 (1993).
313. M. J. Duer, *Ann. Rep. NMR Spectrosc.*, **43**, 1 (2000).
314. J. Jeener, B. H. Meier, O. Bachman and R. R. Ernst, *J. Chem. Phys.*, **71**, 4546 (1979).
315. N. Boden, In "*The Plastically Crystalline State*: *Orientationally Disordered Crystals*", J. N. Sherwood, Ed., John Wiley & Sons, Chichester, 1979, Chapter 5.